2017

Discovery and Characterization of Cytomegalovirus Inhibitors using Reporter-based Antiviral Assays

amine ourahmane

Discovery and Characterization of Cytomegalovirus Inhibitors

using Reporter-based Antiviral Assays

by

Amine OURAHMANE, MS

A thesis submitted in partial fulfillment of the requirements for the degree of

Master of Science at Virginia Commonwealth University.

Virginia Commonwealth University, August 2017

Major Director: Michael McVoy, Ph.D.

Professor, Departments of Pediatrics and Microbiology & Immunology

TABLE OF CONTENTS

LIST OF FIGURES

ABSTRACT

DISCOVERY AND CHARACTERIZATION OF CYTOMEGALOVIRUS INHIBITORS
USING REPORTER-BASED ANTIVIRAL ASSAYS

By Amine Ourahmane, MS

A thesis submitted in partial fulfillment of the requirements for the degree of Master of Science
at Virginia Commonwealth University.

Virginia Commonwealth University, August 2017

Major Director: Michael McVoy, Ph.D.
Professor, Department of Pediatrics and Microbiology and Immunology

Human cytomegalovirus (HCMV), a member of the herpesvirus family, causes

significant disease in immunocompromised patients and is the major infectious cause of birth

defects when acquired congenitally. Current HCMV antivirals are suboptimal due to modest

potency, significant toxicities, and emergence of resistance. Because HCMV does not infect non-

human species, related animal cytomegaloviruses are used as animal models. Of the small animal

cytomegaloviruses only guinea pig cytomegalovirus (GPCMV) has been found to cross the

placenta to cause fetal infection and disease. Thus, the GPCMV/guinea pig model of congenital

infection can be used to study the effectiveness of vaccines or small molecule inhibitors in

preventing or treating congenital infections. However, not all antivirals that inhibit HCMV are

active against GPCMV.

In Aim 1 of the current studies a luciferase-based assay was developed and used to

determine the sensitivity of GPCMV to three novel inhibitory compounds, BDCRB, BAY 38-

4766, and letermovir, which block DNA maturation of HCMV by targeting the viral terminase

complex. BDCRB and BAY 38-4766 were active against GPCMV.Unfortunately, letermovir,

which recently completed phase 3 clinical testing, was not active against GPCMV at concentrations up to 100 μM.

In Aim 2 the mechanism of action of BDCRB against GPCMV was explored by characterizing an L406P mutation in the GP89 terminase subunit that had been previously identified in a BDCRB-resistant GPCMV. *In silico* homology modeling was used to identify the location of the L406P mutation in a predicted 3-D structure of GP89. That it was not located near a putative BDCRB-binding pocket (which was predicted based on confirmed resistance mutations in the homologous HCMV UL89 subunit) suggested that L406P may not confer BDCRB resistance in GPCMV. That L406P does not confer BDCRB resistance was confirmed by genetic transfer of the L406 mutation into an otherwise wild type GPCMV background and demonstration, using the luciferase-based assay, that the IC_{50} of BDCRB was not significantly altered (*i.e*., the virus containing the L406 mutation was not resistant to BDCRB).

In Aim 3 a green fluorescent protein-based assay was used to evaluate four candidate compounds for antiviral activity against HCMV. These highly positively charged compounds, TriplatinNC, DiplatinNC, [Pt(dien)(Xan)]2+ and Werner's Complex, were hypothesized to interfere with viral binding to cell surface glycosaminoglycans and thereby interfere with viral attachment and subsequent entry.

I. INTRODUCTION

Human cytomegalovirus and human disease

Human cytomegalovirus (HCMV), also known as human herpes virus 5, belongs to the family *Herpesviridae*. Derived from the Greek word *herpin*, meaning to creep, that reflects the creeping or spreading nature of the skin lesions caused by the prototype virus, herpes simplex virus. The *Herpesviridae* family is divided to into three subfamilies: alphaherpesvirinae, bethaherpesvirinae, and gammahepesvirinae, and includes eight human pathogens (7). HCMV is classified in the subfamily betaherpesvirinae, genus cytomegalovirus, type species human herpesvirus.

HCMV is a common virus infection that can transmit through contact with body fluids, including saliva, semen, breast milk, and urine (6). HCMV has a ubiquitous distribution, infecting between 60−100% of adults worldwide. Seroprevalence in the United States is 60% or more, while seroprevalence of 90% or more occurs in South America, Africa, and Asia. By the age of 80 nearly everyone has acquired a HCMV infection. Even though HCMV is mostly asymptomatic in immunocompetent individuals, some individuals show mild fever or mononucleosis-like symptoms. Like other herpesviruses, after initial infection HCMV establishes a latent infection for the entire lifetime of the host. HCMV can cause significant disease in immunocompromised patients, and in the developed world is the most common cause of congenital infections, leading to mental retardation and hearing loss in newborns (6,7). There is no licensed vaccine and available therapeutics are not suitable for use during pregnancy.

HCMV in transplant patients. HCMV is the most common viral infection and the major cause of mortality and morbidity in bone marrow and solid organ transplantation

recipients. Approximately 80-90% of all transplant recipients develop symptomatic HCMV infection with an estimated mortality rate of 5% due to the opportunistic behavior of the HCMV under immunosuppression (9). The type of organ transplanted plays a role in the severity of the infection. Small intestine, pancreas, and lung transplant recipients are at higher risk of acquiring HCMV infection than kidney, heart, and liver transplant recipients (10). Recipients who develop a primary infection after transplantation are at high risk for symptomatic disease such as hepatitis, fever, GI ulcers, and pneumonia, with severity that ranges from mild to life-threatening. HCMV disease can also occur after reactivation from latency in seropositive transplant recipients. HCMV infection can cause an additional immunosuppression that results in increased risk for fungal and other opportunistic infections (11). Several diseases are related to HCMV infection following transplantation, such as constrictive bronchiolitis syndrome subsequent to lung transplantation, accelerated coronary atherosclerosis after heart transplantation, transplant rejection, transplant dysfunction, vanishing bile duct syndrome after liver transplantation, constrictive bronchiolitis syndrome after lung transplantation, and the development of post-transplant lymphoproliferative disease (12).

HCMV among AIDS patients. HCMV is a frequent opportunistic pathogen complicating human immunodeficiency virus (HIV) and AIDS patients. More than 45% of patients with AIDS are aggrieved with HCMV disease at some point through the course of their AIDS disease. The most common effects of HCMV infection are gastrointestinal infection, retinitis, and neurologic disease. About 85% of all patients with AIDS acquire HCMV retinitis that can progress to total retinal destruction and blindness if untreated (13). While HCMV infection in HIV/AIDS patients has become less common following the development of highly

active antiretroviral therapy, nevertheless the long-term consequences of HCMV infection in AIDS patients is still indeterminate (14).

Congenitally infected fetuses. In the United States HCMV is the leading cause of congenital viral infection. Approximately 1% of all live births each year (~ 40,000) are born with an active HCMV congenital infection. However, only 20% (~8,000) of these are symptomatic at birth. This makes HCMV the most common infectious disease that can cause morbidity and mortality in infants (15). HCMV infection either occurs in *utero* by transmission from mothers who experienced a recent primary infection, a reinfection, or a reactivation of a latent infection (16). Newborns can also be infected peri- or post-natally by contacting the blood or other secretions such as breast milk or saliva of seropositive women (17). HCMV congenital infections can cause damage to the organs of perception and impairment to the central nervous system. Symptomatic newborns may have mental retardation, cerebral palsy, hearing deficit, vision impairment, microcephaly, encephalopathy, chorioretinitis, seizures or hepatosplenomegaly (18). An additional 15% of infants who are infected but apparently asymptomatic at birth will later develop HCMV-associated hearing loss and mental retardation (34).

The HCMV Life Cycle (Figure 1)

HCMV has a large double-stranded linear 235-kb DNA genome encoding over 200 genes. The genome is packaged within a 100-nm diameter (8) enveloped icosahedral capsid surrounded by a protein matrix tegument and a lipid bilayer envelope. The latter contains numerous viral surface glycoproteins such as glycoproteins B, H, L, M, N, and O. These surface glycoproteins function in virus-cell binding and entry of the virus into host cells (9).

HCMV enters human cells by direct fusion or through the endocytic pathway. Capsids are released into the cytoplasm and translocated via microtubules to nuclear pores, where the viral DNA is ejected into the nucleoplasm. The genome then circularizes and initiates gene expression in three different phases, producing three different classes of proteins: immediate-early, early, and late. Immediate-early proteins are the first to be expressed. They contribute with other cellular transcription factors to regulate the expression of early and late genes. Early viral genes produce proteins involved in viral DNA synthesis, DNA repair, and immune evasion. Late proteins encode virus structural proteins essential for virion assembly, including envelope glycoproteins, tegument proteins, and capsid proteins. Late proteins are expressed only after the replication of viral DNA (8).

Following early protein expression viral DNA replication occurs by what is believed to be a rolling circle mechanism, producing large concatemers of dsDNA linked in a head-to-tail fashion. Once DNA replication has initiated, capsid proteins are expressed and are translocated to the nucleus where they self-assemble into procapsids. Concatemeric viral DNA is inserted into the procapsids and cleaved by the viral terminase. The resulting nucleocapsids then bud through the inner nuclear membrane, followed by a de-envelopment at the outer nuclear membrane. Once in the cytoplasm, capsids undergo further maturation by gaining tegument proteins and their final glycoprotein-containing envelope as they bud into cytoplasmic vesicles. Mature progeny virions are released to the extracellular environment by exocytosis.
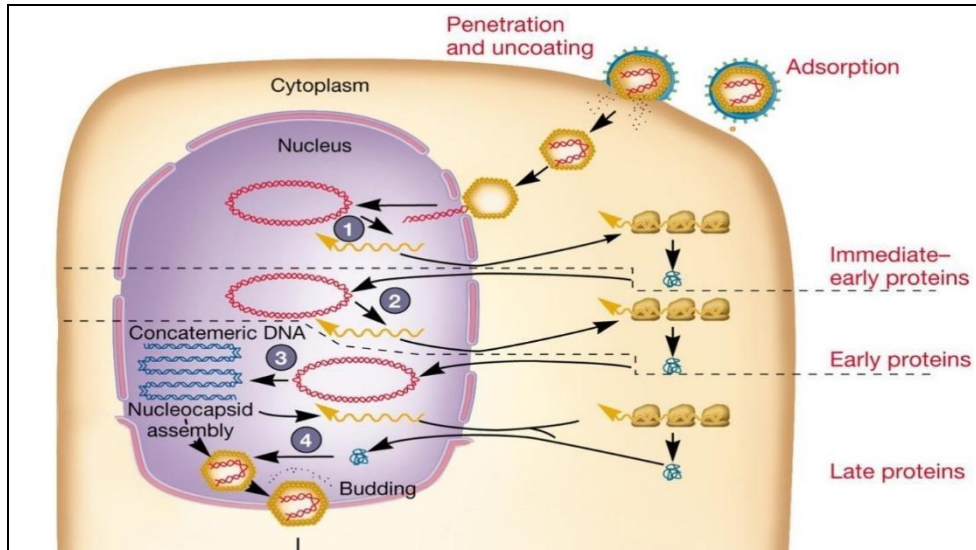
Figure 1: Life cycle of herpesviruses

HCMV Antivirals

At the present time, there are only four drugs commonly used for the treatment of HCMV infections: ganciclovir (and its oral prodrug valganciclovir), foscarnet, and cidofovir (Figure 2). Each of these drugs is used to treat certain HCMV complications by targeting the viral DNA polymerase (Figure 3). However, these therapies are insufficient and have limitations of modest efficacy, toxicity, and risk of development of resistance. These drugs are not approved to treat congenital HCMV infections during pregnancy (19).
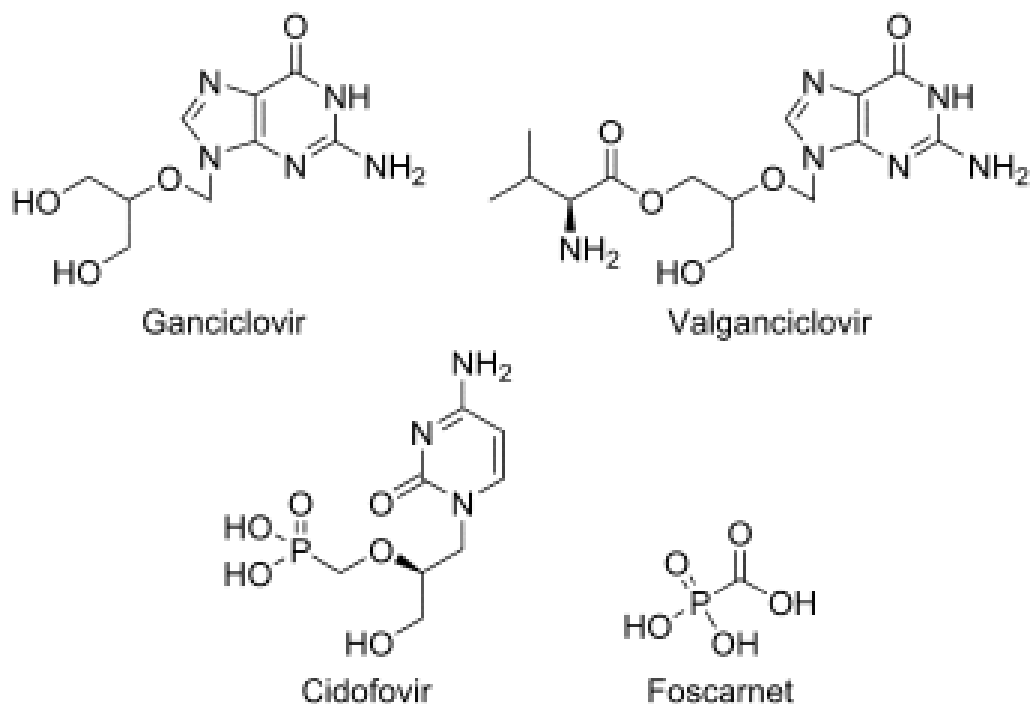
Figure 2: Currently licensed HCMV drugs.

Ganciclovir. Ganciclovir, or DHPG (9-(1,3-dihydroxy-2-propoxymethyl) guanine), is commonly used to treat several viruses belonging to the herpesvirus family. It was the first drug to be approved to treat HCMV infection and remains the drug-of-choice for HCMV infection and HCMV disease in AIDS and transplant recipients (20). Ganciclovir is a synthetic analog of 2'-deoxyguanosine (Figure 2). It is first phosphorylated by the viral kinase pUL97 to its monophosphate form, and then to its di- phosphate and tri-phosphate form by host cell kinases.(Figure 3) The tri-phosphate form is a deoxyguanosine triphosphate (dGTP) analog that competitively inhibits the incorporation of dGTP by the viral DNA polymerase (pUL54). Incorporation results in slowing down of viral DNA synthesis (21). Mutations in either the pUL97 kinase or the pUL54 viral DNA polymerase can lead to resistance to ganciclovir (22). Even tough it is the drug-of-choice, ganciclovir cannot be prescribed to all patients because of problems of toxicity, such as in renal transplant patients, in which ganciclovir can cause kidney

failure because its levels increase in the renal cortex (23). Ganciclovir is also carcinogenic and teratogenic, and thus, it cannot be used by pregnant women (24). The major toxicity is neutropenia, which requires frequent monitoring of neutrophil counts (19).

Foscarnet. Foscarnet, or phosphonoformic acid, was the second drug approved by the FDA as a second line therapy against HCMV infection. It is usually prescribed for patients who develop resistance against ganciclovir. Foscarnet is a pyrophosphate analog (Figures 2, 3) and blocks the pyrophosphate binding site in the viral DNA polymerase. This inhibits the release of pyrophosphate from the terminal nucleoside triphosphate on the growing DNA chain, and thereby inhibits the function of the viral DNA polymerase. Foscarnet can be used to treat patients who develop ganciclovir resistance in UL97, and patients in which ganciclovir cannot be used because of its toxic effects (24,25).

Cidofovir. Cidofovir, or 1-[(S)-3-hydroxy-2-(phosphonomethoxy) propyl] cytosine dihydrate (Figure 2), was the third drug approved to treat HCMV infections, and also can be used against other herpesviruses. Cidofovir is an acyclic nucleoside phosphonate. The host cell kinases convert the acyclic nucleoside phosphonate to an active diphosphate (Figure 3). In this active form cidofovir acts as a competitive inhibitor to deoxycytosine triphosphate and incorporates into the viral DNA. As it lacks a 3' OH it inhibits viral DNA polymerase function by causing chain termination. Unlike ganciclovir, cidofovir does not involve the function of UL97. Thus, only mutations in UL54 DNA polymerase can cause resistance. Cidofovir is a carcinogen and teratogen, and therefore cannot be used during pregnancy (24,25).
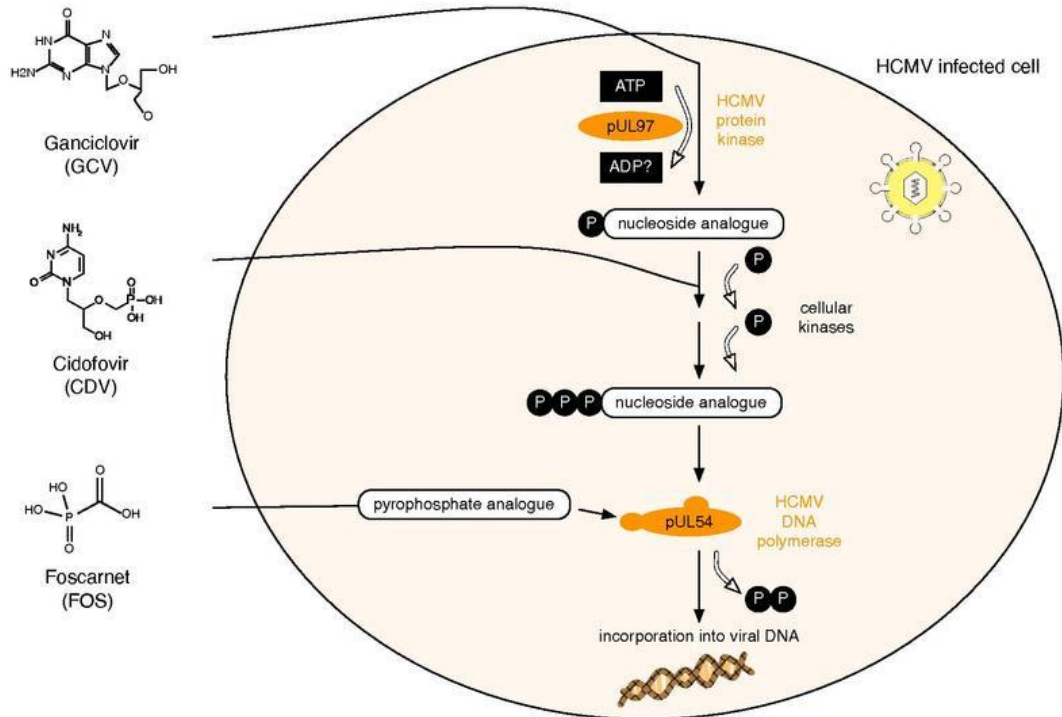
Figure 3: Mechanism of action of HCMV drugs: (1) Ganciclovir is a synthetic analog of 2'-deoxyguanosine. It is first phosphorylated by the viral kinase pUL97 to its monophosphate form and then to its di- phosphate and tri- phosphate form by host cell kinases. Ganciclovir triphosphate competitively inhibits the incorporation of dGTP by the viral DNA polymerase (pUL54), resulting in slowing down of viral DNA synthesis. (2) Host cell kinases convert cidofovir to an active diphosphate form that acts as a competitive inhibitor to dCTP and incorporates into the viral DNA, causing chain termination. (3) Foscarnet is a pyrophosphate analog that blocks the pyrophosphate binding site of HCMV DNA polymerase and inhibits the release of pyrophosphate from the terminal nucleoside triphosphate on the growing DNA chain, resulting of inhibition of the viral DNA polymerase.

HCMV DNA packaging

All currently licensed HCMV antivirals block viral DNA synthesis. The process by which newly synthesized viral DNA is packaged into capsids and cleaved, mediated by the viral terminase complex, has emerged as an attractive target for development of new antivirals. The HCMV terminase is believed to be a three-subunit complex consisting of UL51, UL56 and UL89. UL89 is believed to have ATPase and endonuclease activity. UL56 has also been reported to have ATPase activity that may provide energy for DNA translocation into the capsid (42). Also, UL56 has been proposed to direct protein-protein interactions of the terminase with the portal protein UL104. The third subunit, UL51, is important for terminase function but has not been well characterized (26).

As illustrated in Figure 4, terminase is thought to associate with concatemer ends and mediate initial docking with the portal of newly formed procapsids. The concatemeric DNA is then transferred through the portal into the procapsid using energy provided by hydrolysis of ATP. When approximately one genome has entered the procapsid, the terminase is authorized to cleave at the next proper cleavage site, which contains *cis* sequences called *pac1* and *pac2*. The capsid is then thought to be stabilized by addition of viral proteins to the vertices, and based on bacteriophage models, a "plug" protein may close off the portal to secure the DNA inside. The mature DNA-containing nucleocapsid is called a C-capsid. Two aberrant and presumably dead-end capsid forms are also abundant in infected-cell nuclei. Empty A-capsids are thought to arise by spontaneous loss of packaged DNA, while scaffold-containing B-capsids are thought to arise by spontaneous scaffold proteolysis in the absence of DNA packaging.
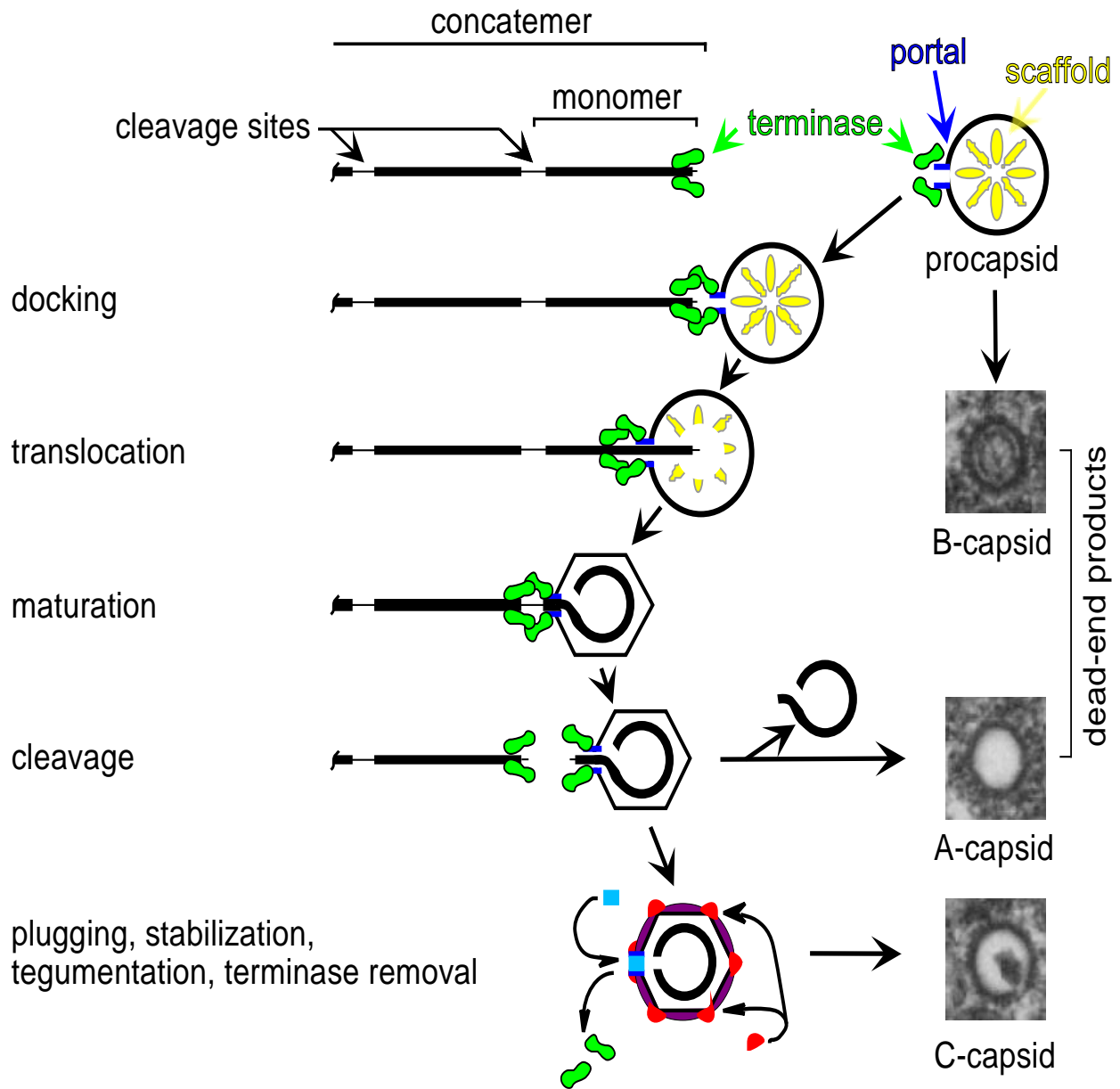
Figure 4: HCMV genome packaging. The concatemer, bound to terminase, docks with a capsid portal and translocates DNA into the procapsid. At the same time, the scaffolding is proteolytically cleaved and exits the capsid. DNA is packaged until a monomer has entered. The capsid angularizes and terminase cleaves the DNA at the appropriate site. The capsid is then sealed and stabilized by addition of viral proteins and the terminase is removed. Images show representative electron microscope of three types of capsids that are found in infected cell nuclei. C-capsids contain DNA, A-capsids appear empty and are thought to arise by spontaneous loss of packaged DNA. B-capsids contain scaffold protein fragments and are thought to arise by spontaneous scaffold proteolysis in the absence of DNA packaging.

10

Terminase inhibitors

      <u>The halogenated benzimidazoles</u>. The halogenated benzimidazoles were discovered in the laboratories of John Drach and Leroy B. Townsend. BDCRB (2-bromo-5, 6-dichloro-1-β-d-riborfuranosyl benzimidazole riboside) (Figure 5) and TCRB (2, 5, 6-trichloro-1-β-d-riborfuranosyl benzimidazole riboside) are members this class. Both inhibit HCMV replication late in the replication cycle without inhibiting viral DNA synthesis (2) and were the first compounds shown to target terminase to prevent concatemeric DNA from being packaged into capsids. HCMV resistance to TCRB and BDCRB was mapped to mutations in UL89 and UL56 (2, 3). These compounds were not pursued for further clinical development because they are cleaved in vivo to produce less active but additional cytotoxic aglycones (33).

      BAY 38-4766 (also known as tomeglovir, or 3-Hydroxy-2,2-dimethyl-*N*-[4({[5-(dimethylamino)-1-naphthyl] sulfonyl} amino)-phenyl] propanamide, Figure 5). BAY 38-4766 is a nonnucleoside that inhibits HCMV with an $IC_{50} = 1.00 \pm 0.40$ μM (28), BAY 38-4766 resistance has been mapped to the murine cytomegalovirus gene encoding M89, a homolog of UL89 (28).

      <u>Letermovir</u> (also known as AIC246, Figure 5). Letermovir is a more recently discovered nonnucleoside that inhibits HCMV with an IC_{50} of 5 nM (26). Resistance maps to UL56 (26). Letermovir recently completed Phase IIb and III trials.
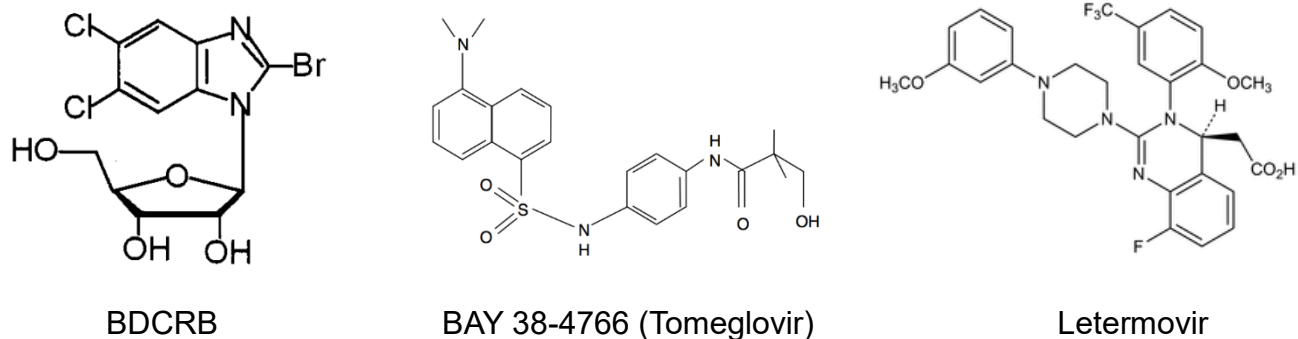
Figure 5: Structures of HCMV terminase inhibitors BDCRB, BAY 38-4766 (Tomeglovir), and Letermovir. (45,46,47)

The guinea pig model of congenital cytomegalovirus infection

Guinea pig is small rodent that has been used about 200 y as model system for human infectious disease (36) because HCMV does not infect non-human species, so it cannot be studied using animal models in vivo. so, animal models must use related animal CMV including mouse CMV, rat CMV, rhesus macaque CMV and Guinea Pig CMV. However, MCMV and RCMV do not cross the placenta to infect the fetus. GPCMV can cross the placenta and cause congenital infection (37)

Genome Structures of HCMV and GPCMV

The genome structures of herpesviruses are frequently complex. The HCMV genome is organized as two regions of unique sequences, unique long (UL) and unique short (US), each bordered by inverted duplications of *b* and *c sequence* repeats that are further flanked by short *a sequence* repeats. There are two genome variants. Type 1 genomes have no *a sequence* at the terminal right end, while type 2 genomes have at least one *a sequence* at the terminal right end (Figure 6). In addition, homologous recombination between *b* and *c sequence* repeats results in inversion of UL and US, producing four genome isomers. This complex mixture of genome

structures greatly complicates molecular analysis of HCMV genomes and replicative intermediates.
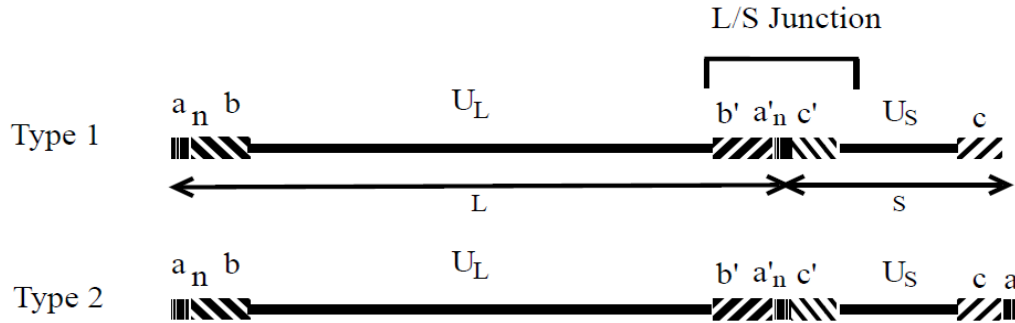
Figure 6: HCMV Genome Structures

The GPCMV genome structure is less complex than that of HCMV. It does not have inverted repeats within the genome and therefore does not form different genome isomers by genome segment inversion. However, the GPCMV genome does have direct (*a sequence*-like) repeats at the terminal ends, and similar to HCMV, it has two genome variants: type 1 genomes have predominantly one terminal repeat at the left end and no terminal repeat at the right end, while type 2 genomes have predominantly one terminal repeat at both ends (Figure 7).
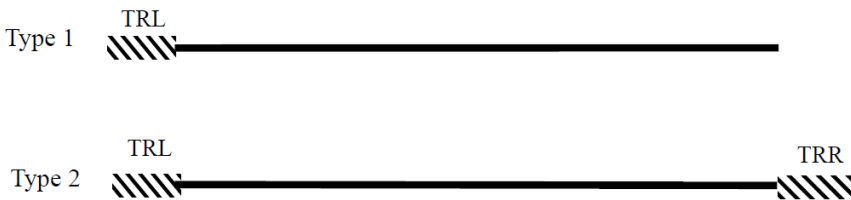
Figure 7: GPCMV Genome Structures. Terminal repeat left (TRL) and terminal repeat right (TRR) are short (1-kb) sequences similar to the *a sequences* of HCMV.

Sensitivity of GPCMV to terminase inhibitors

BDCRB. Previous studies by our laboratory showed that BDCRB has the ability to inhibit GPCMV with an IC_{50} of 4.7 µM (Figure 8) (4). While somewhat less sensitive than HCMV, which has a reported IC_{50} of 1.22 ± 0.27 µM (28), effective inhibitory concentrations of 20-50 µM are well below the cytotoxicity of this compound. Unlike HCMV, BDCRB does not stop the formation of monomeric GPCMV DNA or its insertion into capsids. However, the packaged DNA is abnormal in three ways. First, it is completely type II at the right end; second, it is shortened heterogeneously, losing 2.7 to 4.9 kb of left-end sequences; and finally, although packaged into capsids, the capsids are not sealed, and fail to protect the DNA from nuclease digestion (4).
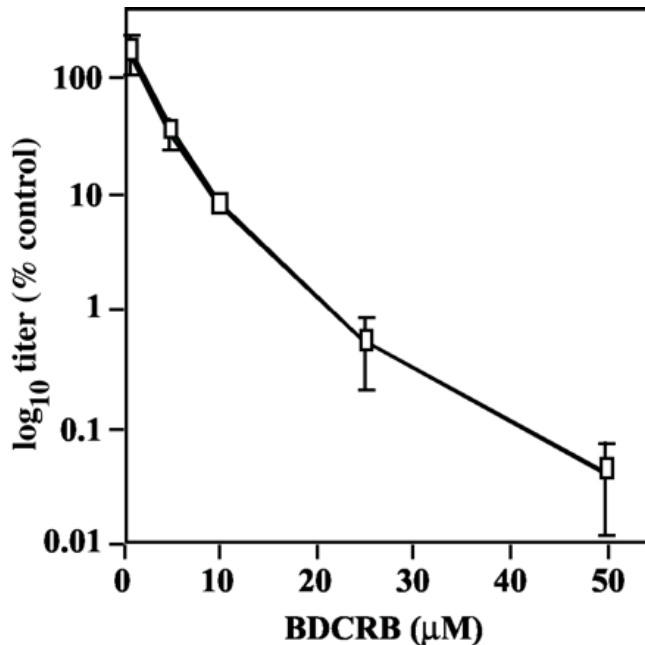
Figure 8: Inhibition of GPCMV replication by BDCRB (reprinted from (4))

BAY 38-4766. In previous studies from our laboratory and that of our collaborator, Mark Schleiss, BAY 38-4766 was shown using a plaque reduction assay to be active against GPCMV with an IC_{50} of approximately 0.5 μM (Figure 9) (27). This is comparable to the sensitivity of 1.21 ± 0.08 μM reported for HCMV (28).
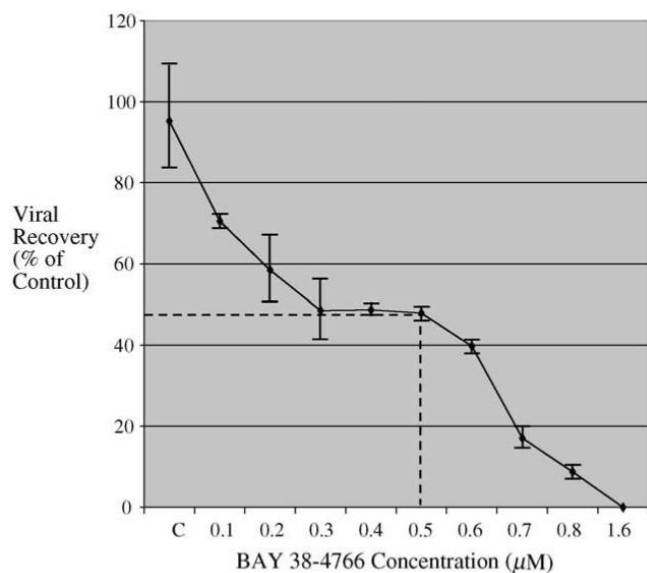
Figure 9: Inhibition of GPCMV by BAY 38-4766 (reprinted from (27)).

Letermovir. Until now it has not been examined if GPCMV is sensitive to letermovir; however, studies show that letemovir is very specific to HCMV and does not inhibit rodent or other human herpesviruses, and demonstrates minimal activity against other human pathogenic viruses (38). Thus, it is possible that GPCMV is not sensitive to letermovir. However, the potential to test

the ability of letermovir to inhibit congenital transmission or fetal disease in the guinea pig model

warrants evaluation of GPCMV for sensitivity to letermovir.
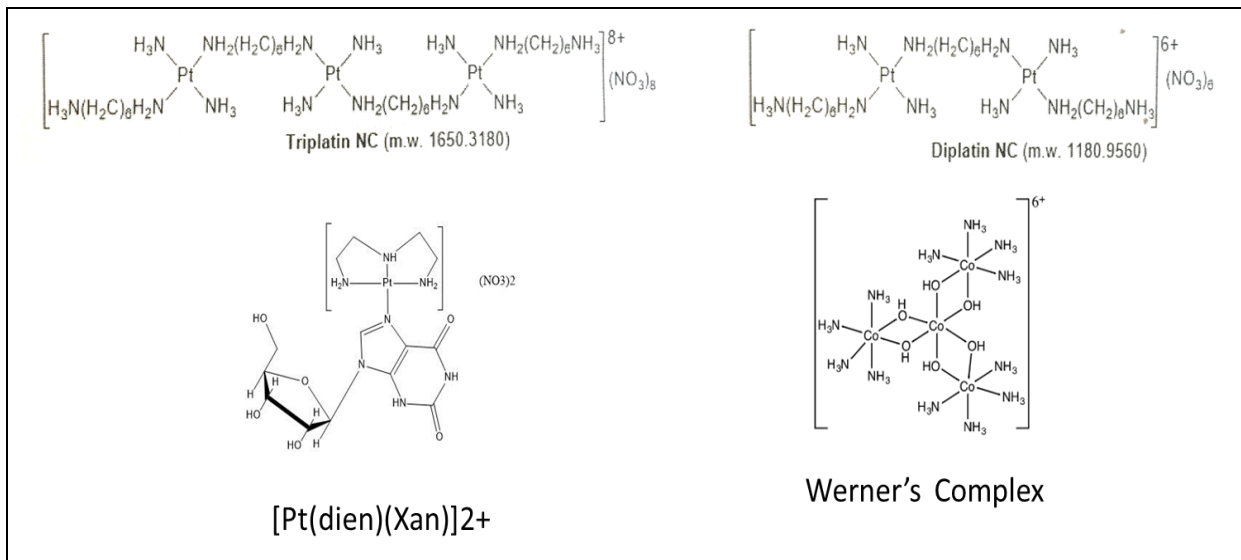
Figure 10: These highly positively charged compounds (Farrell et al.unpublished)

Research Aims

Aim 1: To develop a luciferase-based antiviral assay for GPCMV and to use this assay to evaluate GPCMV sensitivity to BDCRB, BAY 38-4766, and letermovir. Previously our laboratory developed a luciferase-based antiviral assay for HCMV and demonstrated that this state-of-the-art technology provides rapid quantitative data for determining antiviral activities (38). Dr. Jian Ben Wang recently constructed a recombinant GPCMV called GPCMV-NanoLuc that contains an expression cassette for NanoLuc® Luciferase. (Wang and McVoy, unpublished)

In Aim 1.1 GPCMV-NanoLuc was used to determine the relationship between multiplicity of infection (MOI), time post infection, and luciferase activity in order to establish conditions in which luciferase activity exhibits a linear relationship with the amount of infectious virus.

In Aim 1.2 this information was used to design an antiviral yield reduction assay in which the ability of different inhibitor concentrations to reduce the amount of virus progeny released into the culture medium was measured using luciferase as a surrogate reporter. This assay was then used to quantitatively measure the antiviral activities of BDCRB, BAY 38-4766, and letermovir against GPCMV.

Aim 2: To determine if a L406P mutation in GPCMV GP89 confers resistance to BDCRB.
BDCRB-resistant GPCMV variant R-75 has multiple genetic changes relative to the BDCRB-sensitive parental virus, one of which is an L406P mutation in terminase subunit GP89 that in the

linear amino acid sequence lies near but not within the region (residues 350-360) where amino acid substitutions have been shown to confer resistance to BDCRB in HCMV (28)

In Aim 2.1, *in silico* structural modeling was used to construct homology-based structural models of UL89 and GP89 based on the crystal structure of bacteriophage T4 terminase large subunit gp17. *In silico* docking was then used to determine probable binding configurations of BDCRB in the region of UL89 residues 350-360. The analogous region of GP89 was then determined and found to be spatially distant from the L406P mutation, suggesting that L406P is unlikely to directly interfere with BDCRB binding to GP89.

In Aim 2.2 *galK* recombineering of the GPCMV-NanoLuc genome, cloned as a bacterial artificial chromosome (BAC) in *E-coli,* was used to insert the L406P mutation into the otherwise wild type genetic background of GPCMV-NanoLuc. The luciferase-based assay was then used to measure the sensitivity of both parental GPCMV-NanoLuc and GPCMV-NanoLuc containing the GP89 L406P mutation. The results indicated that the L406P mutation does not confer significant resistance to BDCRB.

Aim 3: To determine the antiviral activities of four highly positively charged compounds against HCMV. The 8+ positively charged compound triplatinNC has been reported to bind negatively charged cell surface glycosaminoglycans (40). As many viruses, including HCMV, are thought to initiate binding to target cells through charge interactions with surface glycosaminoglycans, triplatinNC and three additional positively charged experimental compounds were hypothesized to inhibit viral entry by binding to and neutralizing negative charges of cell surface glycosaminoglycans66.

In Aim 3.1 a green fluorescent protein (GFP)-based spread inhibition assay was used to determine the HCMV-inhibitory activities of four charged compounds, TriplatinNC, DiplatinNC, Pt(dien)Xan, and Werner's Complex. DiplatinNC and Werner's Complex were found to have HCMV inhibitory activities with IC_{50}s of 5 and 4 μM, respectively.

In Aim 3.2 cytotoxicities of DiplatinNC and Werner's Complex were measured using a luciferase-based CellTiter-Glo® cell viability assay. The 50% toxicity (TC_{50}) values for both Werner's Complex and DiplatinNC were significantly higher than the IC_{50}s for antiviral activity against HCMV, suggesting that both compounds have specific anti-HCMV activities.

II. MATERIALS AND METHODS

Cells

Human MRC-5 fetal lung fibroblasts (ATCC CCL-171) and guinea pig lung fibroblasts (GLF) (ATCC® CCL-158) were obtained from American Type Culture Collection and cultivated in high glucose Dulbecco's modified Eagle medium (Life Technologies) supplemented with 10% heat-inactivated fetal bovine serum (FBS) (Life Technologies), 10,000 IU/L penicillin, 10-mg/L streptomycin sulfate, and 29.2 mg/mL L-glutamine (Life Technologies) (DMEM). All cell cultures were maintained at 37°C in a 5% CO_2 atmosphere.

Viruses

HCMV BAD*r*UL131-Y4, a gift from Dai Wang and Thomas Shenk, was derived from a BAC clone of the HCMV strain AD169 genome that had been modified in *E. coli* by Wang and Shenk to contain a GFP reporter cassette (29). GPCMV-NanoLuc was derived from BAC clone N13R10-r129 (41), an infectious BAC clone of GPCMV strain 22122, after modification in *E. coli* to contain an expression cassette for NanoLuc® Luciferase (Wang and McVoy, unpublished). HCMV BAD*r*UL131-Y4 was adjusted to 0.2 M sucrose, with a titer of 1 x 10^5 and stored at -80°C. GPCMV-NanoLuc was adjusted to 0.2 M sucrose, with a titer of 1.84 x 10^6, and stored in liquid nitrogen.

Inhibitory compounds

BDCRB was a gift from John Drach and Leroy Townsend (University of Michigan) (30). BAY 38-4766 was provided by Bayer® Pharmaceuticals (Tubigen, Germany). Letemovir was provided by Merck Sharp & Dohme Corp. (West Point Pennsylvania, USA). BDCRB was

dissolved in DMSO at a stock concentration of 100 mM. BAY 38-4766 and letemovir were dissolved in DMSO at a stock concentration of 50 mM. Werner's Complex, TriplatinNC, DiplatinNC, and Pt(dien)Xan were gifts from Nicholas P. Farrell (Virginia Commonwealth University). TriplatinNC, DiplatinNC, and Pt(dien)Xan were dissolved in water at a stock concentration of 1 mM. Werner's Complex was dissolved in HCl pH of 2, at a stock concentration of 1 mM.

Modeling

HHpred (server) was used to detect protein homology to UL89 and GP89. Both models were constructed based on the crystal structure of bacteriophage T4 gp17, which was the most similar terminase subunit for which a crystal structure is available. Moddler was used to generate 200 models for both proteins, then one model was chosen based on the lowest energy. GOLD software was used to dock the BDCRB to a pocket in corresponding to know BDCRB resistance mutations UL89, and then the HINT (Hydropathic INTeractions) scoring was used to evaluate the UL89 BDCRB interaction. The SYBYL®-X was used for modeling and simulation.

galK Recombineering

BAC N13R10r129-NanoLuc was constructed by Jian Ben Wang (Wang and McVoy, unpublished). It was modified from BAC clone N13R10, which contains the complete GPCMV strain 22122 genome (31), first to repair a frame-shift mutation in GP129 (42), and subsequently to contain an expression cassette for NanoLuc® Luciferase. Two-step galactokinase recombineering in *E. coli (32)* was used to modify N13R10r129-NanoLuc to contain a single amino acid L406P substitution in GP89.

In the first step, nucleotides 156635 to 156654 of BAC N13R10r129-NanoLuc were replaced with a *galK* expression cassette encoding galactokinase. Synthetic oligonucleotides GP89-406-galk-FW (CACGTTCATCACCATCAGCTCGGAGGTGCGGAGGACCGCCAACATGTTCACGACTC ACTATAGGGCGAATTGG) and GP89-406-galk-RV (TCCGAGATCTTGTTGGTGCCCCCCATGATCTCGTCCATGAAGGAACCCGCGCTATGA CCATGATTACGCCAAGC) were used to PCR amplify the *galK* expression cassette from plasmid pGalK to produce a product containing the *galK* expression cassette flanked by 50-bp homologies to the desired insertion site within *GP89*. The product was purified using a PCR purification kit (Qiagen) and restricted with DpnI (New England Biolabs) to digest residual template pGalK DNA (produced in methylation-competent *E. coli*). The PCR product was then size-purified by agarose electrophoresis and isolated using a gel extraction kit (Qiagen).

E. coli strain SW102 containing BAC N13R10r129-NanoLuc was inoculated into Luria-Bertani broth (LB) containing 12.5 µg/ml chloramphenicol and incubated with shaking at 32°C overnight. The following day, 5 mL were transferred into 250 mL LB containing 12.5 µg/ml chloramphenicol and incubated with shaking at 32°C until an optical density at 600 nm of 0.55-

0.6 was reached. 10 mL of the culture was then transferred to a 75-cm^2 tissue culture flask and heat shocked at 42°C for exactly 15 min. in a shaking water bath. The flask was then placed in a horizontal position in an ice/water slurry for 5 min. The cells were transferred to a 15 mL conical tube, pelleted at 5,000 rpm at 4°C for 5 min., washed twice with ice cold water, resuspended in glycerol to a final volume of 50 μl, and incubated overnight at 4°C.

The heat-induced electrocompetent *E. coli* were mixed with 50-100 ng of the PCR product described above and transferred to a 0.1 cm electroporation cuvette (Bio-Rad) that was pre-chilled on ice. The cells were electroporated at 25 mF, 175 kV with Bio-Rad MicroPulser (program EC1), then diluted in 1 mL LB and incubated at 32°C for 2 h. Cells were then pelleted at 13,200 RPM for 15 s, washed twice with 1 mL of M9 salts, and resuspended to a final volume in 100 μl in M9 salts. 100 μl of cells were spread on Gal-positive selection plates consisting of M9 salts, galactose, and 12.5 μg/ml chloramphenicol as described elsewhere (32), and incubated at 32°C until colonies were visible (2-3 days). Colonies were screened using three PCR reactions: (1) primers galk-test3 (GCTGTCGTCATCATCAACAG) and 89ex2-3'-FW

(CGATGGATTGCTTGATGATGC); (2) primers galk-test1 (GGTTATACGTGAACACGACG) 89ex2-3'-RV (AAAGAGTGTAAGGTCCCGTCGG)

; (3) primers 89ex2-3'-FW and 89ex2-3'-RV. Reactions 1 and 2 overlap the left and right breakpoints, respectively, between the *galK* insertion and flanking *GP89* sequences and will only produce products of appropriate size from BACs in which *galK* has correctly inserted. Reaction 3 flanks and overlaps the *galK* insertion and will produce a 420-bp product when no insertion has occurred and a 1.9-kb product when *galK* has correctly inserted. Based on the results from these PCR reactions one BAC clone was selected and designated BAC N13R10_ galk.

In the second step, counter selection was used replace the *galK* insertion with *GP89*

sequences that either restore a wild type GP89 sequence or encode a mutant GP89 containing the

L406P mutation. Two methods were used to generate the necessary DNA sequences. In the first

method, PCR primers GP89-406-Flank FW (TGCTTTCTGACCAGACTGAGCAAC) and

GP89-406-Flank RV (GCTGATTTTTGTACGTCCCCACC) were used to amplify 420-bp PCR

products from GPCMV WT DNA (containing wild type *GP89* sequence) or from GPCMV R75

DNA (containing *GP89* sequences encoding the L406P mutation). In the second method, 100-bp

synthetic oligonucleotides were ordered with 20-bp complementary 3' overlaps. One pair

contained wild type *GP89* sequences flanking the *galK* insertion: GP89-406(WT)-FWAN

(GGACGCCACGGCCTGCCCGTGCTACCGGCTGCACAAGCCCACGTTCATCACCATCA

GCTCGGAGGTGCGGAGGACCGCCAACATGTTCCTGGCGGGTTCC) and GP89-

406(WT)-RVAN

(AACTCCTCGCGGCCGTCGTCCGTGATCAGCACTGTCTCCTCCGAGATCTTGTTGGTG

CCCCCCATGATCTCGTCCATGAAGGAACCCGCCAGGAACATGT). The second pair

contained mutant GP89 sequences flanking the *galK* insertion: GP89-406(P)-FWAN

(GGACGCCACGGCCTGCCCGTGCTACCGGCTGCACAAGCCCACGTTCATCACCATCA

GCTCGGAGGTGCGGAGGACCGCCAACATGTTCCCGGCGGGTTCC) and

 GP89-406(P)-RVAN

(AACTCCTCGCGGCCGTCGTCCGTGATCAGCACTGTCTCCTCCGAGATCTTGTTGGTG

CCCCCCATGATCTCGTCCATGAAGGAACCCGCCGGGAACATGT). The two primer pairs

were used without additional template DNA in PCR reactions described above two generate 180-

bp products containing wild type or mutant *GP89* sequences. Both 420-bp and 120-bp PCR

products were gel purified as described above.

E. coli strain SW102 cells containing BAC N13R10_ galk were heat-induced and rendered electrocompetent as described above. Cells were mixed with 50-100 ng PCR product and electroporated as described above, then diluted in 8 ml LB and incubated with shaking for 4.5 h at 32°C. 1 mL of culture was washed twice in M9 salts, resuspended to final volume in 100 μl M9 salts, spread on Gal counter selection plates consisting of M9 salts, 0.5 μg/ml 2-deoxygalactose, and 12.5 μg/ml chloramphenicol, as described elsewhere (32), and incubated at 32°C. Colonies were screened using PCR reaction 3 (above) to identify colonies that produced a 420-bp product, indicating removal of the *galK* insertion. Selected candidates were confirmed by targeted sequencing of the 420-bp products. After removal of the two PCR primers using a PCR purification kit (Qiagen), 8 μl of each PCR product was mixed in separate reactions with 4 μl of either GP89-406-Flank FW or GP89-406-Flank RV primers and sequenced by Sanger dideoxy sequencing (eurofins Genomics) (32). Following sequence confirmation, two representative BAC clones were selected and designated N13R10r129-NanoLuc _WT and N13R10r129-NanoLuc _exon89_L406P. Although additional BAC clones were derived following transformation with the 420-bp PCR products, the two BAC clones that were selected were both constructed using the 120-bp PCR products described above.

Virus reconstitution

   E. coli containing BACs N13R10r129-NanoLuc _WT or N13R10r129-NanoLuc _exon89_P406L where diluted in 250 mL of LB with chloramphenicol and cultured overnight with shaking at 32°C. BAC DNA was purified using NucleoBond AX BAC DNA purification kits (k3008-1, Biosciences) and eluted in a final volume of 0.4 mL sterile TE or water. GLF cells were seeded into 6-well (35-mm) plates and transfected the next day after they became 60% to 90% confluent. One μg pCre plasmid DNA (to excise the BAC origin), 60 μL of Effectene buffer, and 2-5 μg of BAC DNA were combined. Seven μL of Enhance Reagent was added and the combination was mixed by pipetting up and down 5 times, then incubated for 5 min. at room temperature. Ten μL Effectene was added and mixed by pipetting up and down 5 times, then incubated for 10 min. at room temperature. GLF cells were washed once with 2 mL DMEM and adjusted to a final volume of 1.5 mL DMEM per well. The BAC DNA/Effectene mixture was mixed with 0.7 mL DMEM and mixed by pipetting up and down. Immediately the mixture was transferred to wells of a 6-well plate that contained GLFs in 1.5 mL DMEM. Cultures were incubated for 24 h at 37°C, then washed once with DMEM and fresh DMEM was added. After 7-10 days characteristic, viral cytopathic effect (CPE) was evident. The culture supernatants were then subjected to limiting dilution in 96-well plates. Wells positive for CPE but negative for GFP from plates in which the majority of wells were CPE negative were selected to isolate GFP-negative viruses in which the BAC origin was excised by Cre recombinase, as described previously (31). Selected viruses were amplified in T75 flasks containing confluent GLFs and cell-free virus stocks were prepared from the culture supernatants, stored, and titrated as described above.

Luciferase-based antiviral assay (GPCMV)

For initial optimizations, black-wall/clear-bottom 96-well plates containing confluent monolayers of GLF cells were infected with GPCMV-NanoLuc at various multiplicities of infection and for various periods of time. To quantitate luciferase activities, 100 μL of culture medium was removed from each well and replaced by 100 μL/well Nano-Glo® Luciferase Assay Reagent (Promega). After incubation for 10 min. at room temperature, relative light units (RLU) were measured using a Biotek Synergy HT Multi-Mode Microplate Reader.

For antiviral assays, clear 96-well plates containing confluent monolayers of GLF cells were infected with GPCMV-NanoLuc (wild type parental), GPCMV-NanoLuc-L406P, or GPCMV-NanoLuc (rescued) at an MOI of 0.006. Eight three-fold serial dilutions of the inhibitor compounds (BDCRB, BAY 38-4766, or letermovir) were prepared in DMEM and added in triplicate to wells containing infected cells. Final inhibitor concentrations ranged from 100 μM to 15.2 nM. Uninfected wells and wells that were infected but contained no inhibitor were included as controls on each plate. After incubation for eight to nine days, 50 μL of culture supernatants from each well were transferred to wells of a black-wall/clear-bottom 96-well plate containing uninfected confluent GLF monolayers. After incubation for 48 h luciferase activities in each well were determined as described above. Prism 5 GraphPad Software was used to determine best-fit four-parameter curves for percent maximum RLU (means of triplicate data) vs. log (inhibitor concentration). Antiviral 50% inhibitory concentrations (IC_{50}) were calculated from the inflection points of the four-parameter curves.

GFP-based antiviral assay (HCMV)

Black-wall/clear-bottom 96-well plates containing confluent monolayers of MRC-5 cells were infected with GFP-tagged HCMV BAD*r*UL131-Y4 at an MOI of 0.1. Eight three-fold serial dilutions of the inhibitor compounds (Werner's Complex, TriplatinNC, DiplatinNC, and Pt(dien)Xan) were prepared in DMEM and added in triplicate to wells containing infected cells. Final concentrations ranged from 100 μM to 15.2 nM for Werner's Complex, DiplatinNC, and Pt(dien)Xan), and from 10 μM to 1.52 nM for TriplatinNC. Uninfected wells and wells that were infected but contained no inhibitor were included as controls on each plate. After nine days of incubation GFP fluorescence was measured in relative fluorescence units (RFU) using a Biotek Synergy HT Multi-Mode Microplate Reader. Antiviral IC_{50} values were determined as described above using RFU instead of RLU.

Luciferase-based cytotoxicity assays

Black-wall/clear-bottom 96-well plates containing confluent monolayers of uninfected GLF or MRC-5 cells were incubated with medium containing eight three-fold serial dilutions of inhibitor compounds (BDCRB, Werner's Complex, TriplatinNC, DiplatinNC, and Pt(dien)Xan) at final concentrations ranging from 100 μM to 15.2 nM for BDCRB, Werner's Complex, DiplatinNC, or Pt(dien)Xan), and from 10 μM to 1.52 nM for TriplatinNC. After eight or nine days (matching the duration of inhibitor exposure in the antiviral assays) 100 μL of culture medium was removed from each well and replaced with 100 μL/well CellTiter-Glo® reagent (Promega). After 10 min. of incubation luciferase activities were measured and 50% toxic concentrations (TC_{50}) were determined as described above for IC_{50} determination.

I. RESULTS

Aim 1: Develop a luciferase-based antiviral assay for GPCMV and to use this assay to evaluate GPCMV sensitivity to BDCRB, BAY 38-4766, and letermovir

<u>Aim 1.1 Development of luciferase-based antiviral assay for GPCMV</u>

The virus yield reduction assay is a powerful technique that can be used to evaluate the effectiveness of antiviral compounds. The use of viruses engineered to express a luciferase reporter is a modern technique that provides rapid quantitative data for antiviral assays and replaces the need to determine, via plaque assay, the production and release of new virus progeny from the infected cells. We used NanoLuc-GPCMV, a recombinant GPCMV recently constructed by Dr. Jian Ben Wang to contain a luciferase (NanoLuc) expression cassette (Wang and McVoy, unpublished), to develop a luciferase-based antiviral assay for GPCMV.

To assess the relationship between MOI, time after infection, and luciferase activity in NanoLuc-GPCMV-infected cells, GLF cells were infected with NanoLuc-GPCMV using a range of MOIs, then luciferase activities were measured at different times post-infection. The results were graphed first to show levels of luciferase activity over time, starting from different MOIs (Figure 11A), and second to show the relationship between luciferase activity and the number of infectious particles that were added to the cells when luciferase was measured at different times post infection (Figure 11B). As seen in Figure 11A, luciferase activities (RLUs) increased exponentially and log(RLU) was highly linear over the first 3-4 days of infection starting with MOIs of 0.025 to 0.1. Higher MOIs (1-4) were linear for 2 days but then plateaued thereafter, suggesting that under these conditions all the cells were infected and reached maximal quantities

of NanoLucby day 2 post-infection . The two lowest MOIs, 0.006 and 0.0125, exhibited a one

day pause and then began to increase exponentially, probably because at these low MOIs only

60-150 cells were initially infected and for the first 24 h they produced levels of NanoLuc that

were below a threshold of detection.

The data analysis in Figure 11B revealed that log(RLU) measurements 24 h or 48 h after

infection display linear relationships over a ~3 log dynamic range with the amount of infectious

virus added to the culture. Because the luciferase signal was significantly stronger at 48 h post

infection vs. 24 h, analysis at 48 h was used to conduct all subsequent luciferase-based yield

reduction assays.

(A) (B)
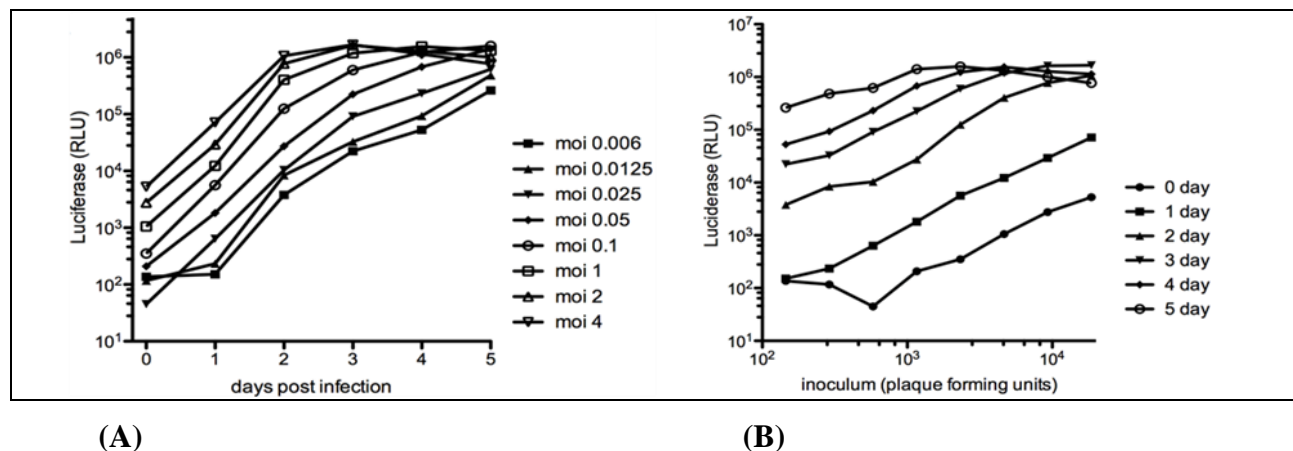
Figure 11: NanoLuc expression after infection with NanoLuc-GPCMV. 96-well plates containing confluent monolayers of GLF cells were infected with NanoLuc-GPCMV virus at the indicated MOIs. Luciferase activities in the wells were determined 3 h (day 0) and on days 1-5 after infection and plotted either vs. time post infection (A) or vs. the amount of infectious virus (plaque forming units) added to each well (B).

Aim 1.2 Evaluating the sensitivity of GPCMV to BDCRB, BAY 38-4766, and letermovir

It has been shown in previous studies that BDCRB and BAY 38-4766 have the ability to

inhibit GPCMV with IC_{50}s of 4.7 μM and 1.0 μM, respectively. (4, 27) These IC_{50}s were

determined based on plaque reduction assays. However, until now it has not been examined if

GPCMV is sensitive to letermovir. The NanoLuc luciferase reporter assay described above was used to re-evaluate the sensitivity of GPCMV to BDCRB and BAY 38-4766 using this new technology, and to determine the susceptibility of GPCMV to letermovir. GLF cells in 96-well plates were infected with NanoLuc-GPCMV at an MOI of 0.006. Medium containing serial dilutions of inhibitors were then added and the cultures were incubated for nine days. To measure the amounts of infectious virus released into the culture medium at that time, 50 μL of culture medium form each well was then transferred to wells containing fresh uninfected GLF cultures. These cultures were then assayed for luciferase activity 48 h after infection. Percent maximum RLU were then plotted vs. log (inhibitor concentration) and IC_{50}s were determined is the inflection points of best-fit four-parameter curves.

The results are shown in Fig. 12. The IC_{50} for BDCRB was determined to be 3.5 μM. This is similar to the IC_{50} of 4.7 μM determined previously by titer reduction (4). Cytotoxicity of BDCRB for GLF cells was determined in parallel by measuring cell viability using the CellTiter-Glo® assay, which uses luciferase activity as measure levels of ATP present in each well.

BDCRB exhibited no significant toxicity (reduction in RLUs) even at the highest concentration tested (100 μM). Thus, the activity of BDCRB against GPCMV is not due to cytotoxicity. The IC_{50} for BAY 38-4766 was 1.1 μM, again comparable to the IC_{50} of 1.0 μM determined previously by titer reduction (27). Finally, the IC_{50} of letermovir was 45 μM, while its reported IC_{50} for inhibition of HCMV is 5 nM (26). While we have not measured the toxicity of letermovir or GLF cells, reported toxicity for human fibroblasts is 30 μM (42). Thus, it appears that the activity of letermovir against GPCMV, which was only observed at the highest concentration of 100 μM, was almost certainly due to cytotoxicity. Therefore, GPCMV does not appear to be sensitive to letermovir.
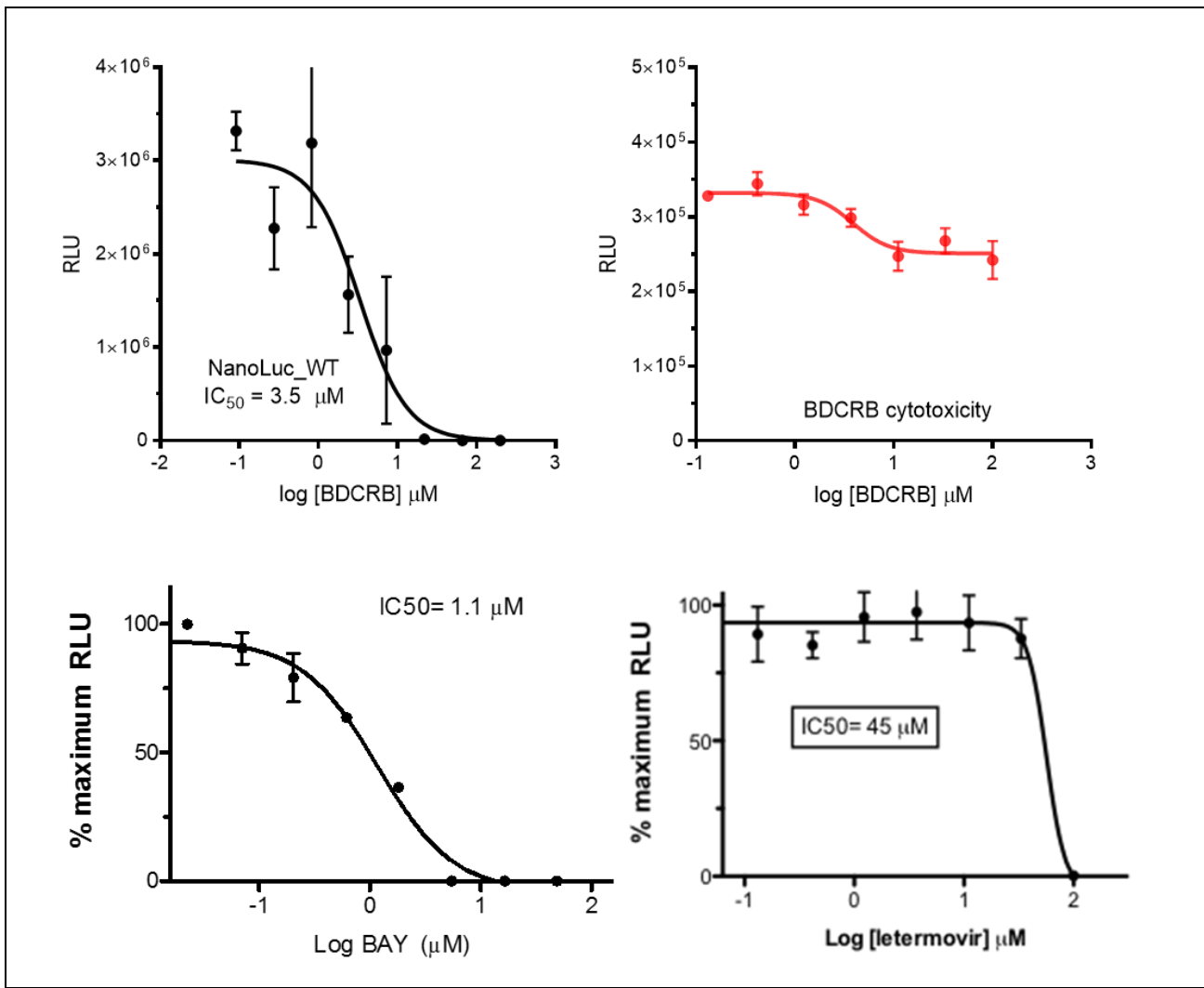
Figure 12: Antiviral activities of terminase inhibitors against GPCMV. GLF monolayers in 96-well plates were infected with NanoLuc-GPCMV (MOI = 0.006) and incubated in the presence of increasing concentrations of inhibitors. After nine days culture supernatants (50 μL) from each well were transferred to wells containing uninfected GLF monolayers and luciferase activities in RLU were measured after incubation for 48 h. RLU were converted to percent maximum RLU and graphed vs. log[BDCRB]. Cytotoxicity (red) of BDCRB was measured by incubating replicate uninfected GLF cultures with the same concentrations of BDCRB for nine days and measuring cell viability in RLU using the CellTiter-Glo® assay. RLU from antiviral and cytotoxicity experiments were converted to percent maximum RLU and graphed vs. log[BDCRB].

Aim 2: To determine if the L406P mutation in GPCMV GP89 confers resistance to BDCRB

Aim 2.1 *in silico* structural modeling of terminase subunits UL89 and GP89

In previous unpublished studies from our laboratory, a BDCRB-resistant GPCMV variant was

produced by passaging the wild type virus for several months in the presence of increasing

concentrations of BDCRB. A clonal virus was isolated by limiting-dilution and confirmed to be

BDCRB-resistant. This BDCRB-resistant virus was named R-75 (Figure 13).
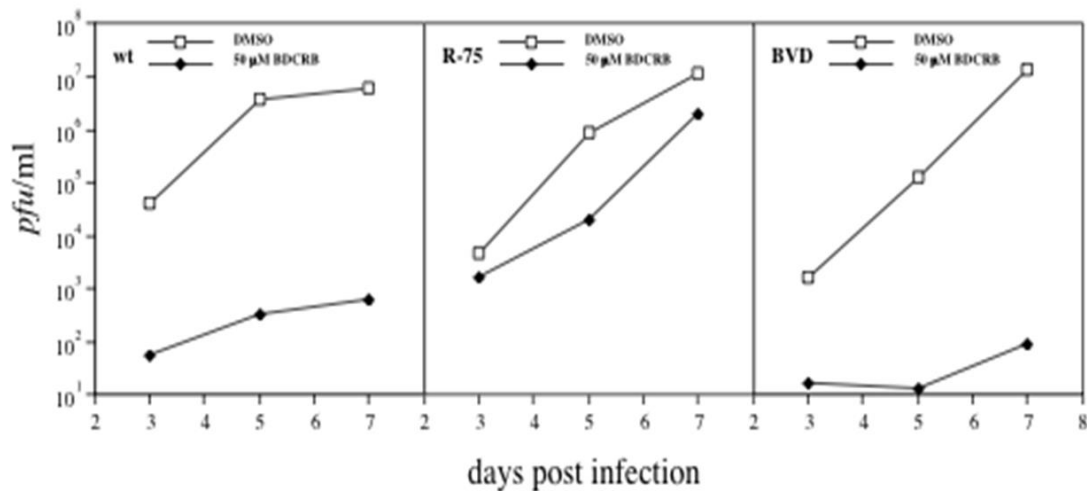
Figure 13: GPCMV resistant to BDCRB. Growth curves were conducted for the indicated viruses in the presence or absence of 50 μM BDCRB. Virus BVD is a control GPCMV that contains a large deletion similar to a deletion in R-75 (Sauer and McVoy, unpublished observations).

Analysis of R-75 revealed three genetic aberrations relative to the parental wild type virus: (1) a

nucleotide change that results in a single L406P amino acid substitution in GP89 terminase

subunit; (2) a large deletion of 12-kb in the HindIII E region of the genome; and (3) an

amplification of the number of terminal repeats at either genomic terminus. It not known which,

if any, of these genetic aberrations are associated with BDCRB resistance of R-75.

In silico homology-based structural modeling was used to predict potential structural models for UL89 and GP89 and then to predict where BDCRB may bind to UL89 based on locations of known BDCRB resistance mutations. Both models were constructed based on the crystal structure of bacteriophage T4 gp17, which was the most similar terminase subunit for which a crystal structure is available.

GP89 and UL89 are believed to have functions in DNA packaging that are similar to those of gp17. The N-terminal half of gp17 is believed to have ATPase activity, while the C-terminal half is believed to have DNA binding and endonuclease activity. The two domains are thought to be connected by a central flexible "hinge" region (Fig. 14A). One proposed mechanism for DNA translocation suggests that gp17 flexes "open" at the hinge region to an extended conformation and the C-terminal domain then binds to the DNA. In coordination with ATP hydrolysis the hinge region then flexes "closed" back to the contracted conformation and pulls the DNA with it. It then releases the DNA and extends again to repeat the cycle. Presumably several gp17 molecules encircle the DNA, interface with the portal, and work sequentially to move the DNA into the capsid (33).

BDCRB-resistance mutations in HCMV UL89 appear to lie at or near this putative hinge region near the middle of the molecule (Fig. 14A, B). Thus, it has been speculated that BDCRB may bind to the hinge region and impair its movement. Interestingly, mutations associated with resistance to BAY 38-4766 also lie near this hinge region (33). Using the homology structure of UL89 a potential BDCRB binding pocket was identified near residues D344 and A355, which confer HCMV resistance to BDCRB when mutated to E and S, respectively (27). The *in silico* docking algorithm GOLD was used determine the most favorable binding configuration of BDCRB in this putative binding pocket (Fig. 14A). The UL89 structure was then modified to

represent UL89 containing the D344E mutations. GOLD analysis then indicated a significant

decrease in the favorability Intuitive Calculations of Free Energy of Binding for Protein-Ligand

Complexes (HINT) was +602 and it significant decrease to -104 in D344E mutations. of BDCRB

binding to the pocket. Thus, the homology-based structural predictions support a model in which

BDCRB binds to the pocket in wild type UL89 but binding is significantly impaired when the

pocket is modified by both substitution, rendering mutant UL89s resistant to BDCRB's

impairment of its functions.

Next, the residues analogous to D344 in UL89 were identified in GP89 and their

locations on the GP89 structural model were used to identify an analogous BDCRB binding

pocket in GP89. GOLD predicted that binding of BDCRB into the GP89 pocket was somewhat

less favorable than for the UL89 pocket, perhaps reflecting the ~5-fold lower sensitivity of

GPCMV to BDCRB compared to HCMV. Importantly, when residue L406 was located on the

GP89 structure, it was clearly not near the putative BDCRB-binding pocket (Fig. 14C). Thus, the

homology-based structural modeling did not support a hypothesis in which the L406P mutation

associated with the BDCRB-resistant GPCMV variant R75 is located in 3-D space near a

potential BDCRB-binding pocket in GP89 that is analogous to the proposed pocket associated

with D344 and A355 in UL89. While not conclusive, these results imply that the L406P mutation

in GP89 may not contribute to the BDCRB resistance of virus R75.
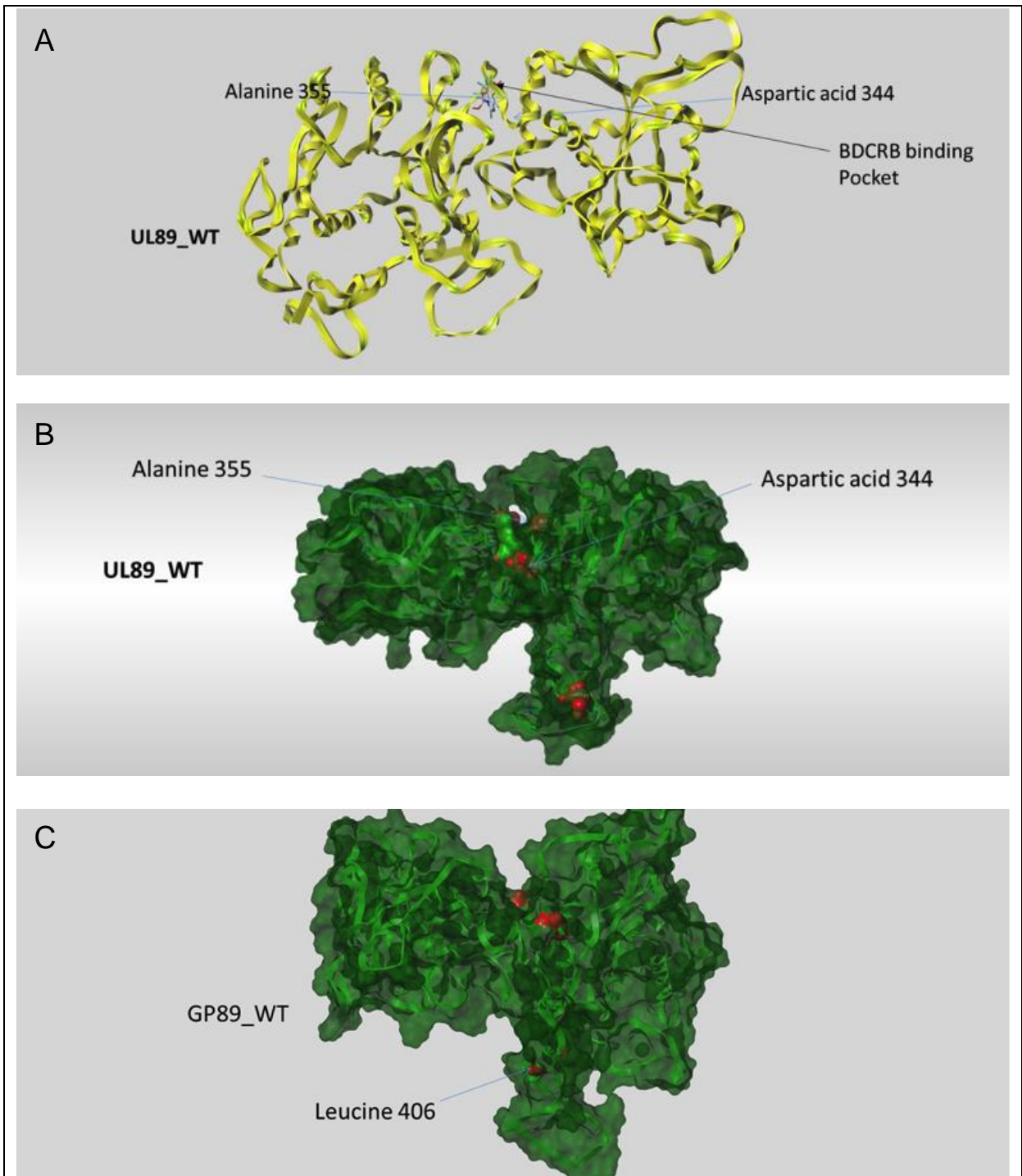
Figure 14: *In silico* generated structural models of UL89 and GP89. Homology models were generated for UL89 and GP89 based on bacteriophage T4 large terminase subunit gp17. (A) Ribbon representation of the UL89 structural model showing BDCRB docked using GOLD into a putative binding pocket defined by residues D344 and A355, which when mutated confer BDCRB resistance in HCMV. (B) Surface representation of UL89 showing D344, A355, and the putative BDCRB-binding pocket. (C) Surface representation of the GP89 structural model showing the GP89 region that corresponds to the putative BDCRB-binding pocket in red. The location of L406 in the 3-D structure is not close to the putative BDCRB-binding pocket.

Aim 2.2 Determine the role of the GP89 L406P in resistance of GPCMV R75 to BDCRB

To determine if the L406P mutation GP89 that occurs in BDCRB-resistant virus R75 is responsible for its resistance to BDCRB, galK recombineering in in *E. coli* was used to insert the L406P mutation into the otherwise wild type BDCRB-sensitive genetic background of NanoLuc-GPCMV. The first step was to design primers to amplify the galK expression cassette in plasmid pGalK and include 50-bp homologies on each primer's 5' end to sequences flanking the L406 codon in the *GP89* gene. The PCR product was then recombined into the BAC-cloned viral genome of NanoLuc-GPCMV using positive selection for galK. In the second step, negative selection against galK was used to remove galK from the BAC and replace it with *GP89* sequences encoding either wild type

GP89 or GP89 containing the L406P mutation. Finally, three viruses were reconstituted by transfection of BAC DNAs into guinea pig cells. The virus NanoLuc-GPCMV-parental was reconstituted from the BAC that was used to construct the *galK* insertion, NanoLuc-GPCMV-R75 was derived by replacing the *galK* insertion with sequences encoding the L406P mutation, and NanoLuc-GPCMV-R75-rescued was derived by replacing the *galK* insertion with wild type *GP89* sequences.

The three viruses were then assayed for sensitivity to BDCRB using the luciferase-based yield reduction assay described above. The IC_{50} for NanoLuc-GPCMV-parental was 3.5 μM, the IC_{50} for NanoLuc-GPCMV-R75 was 5 μM, and IC_{50} for NanoLuc-GPCMV-R75-rescued was 3 μM (Fig. 15). These results conclusively demonstrate that the L406P mutation in GP89 does not contribute significantly to the BDCRB resistance of virus R75.

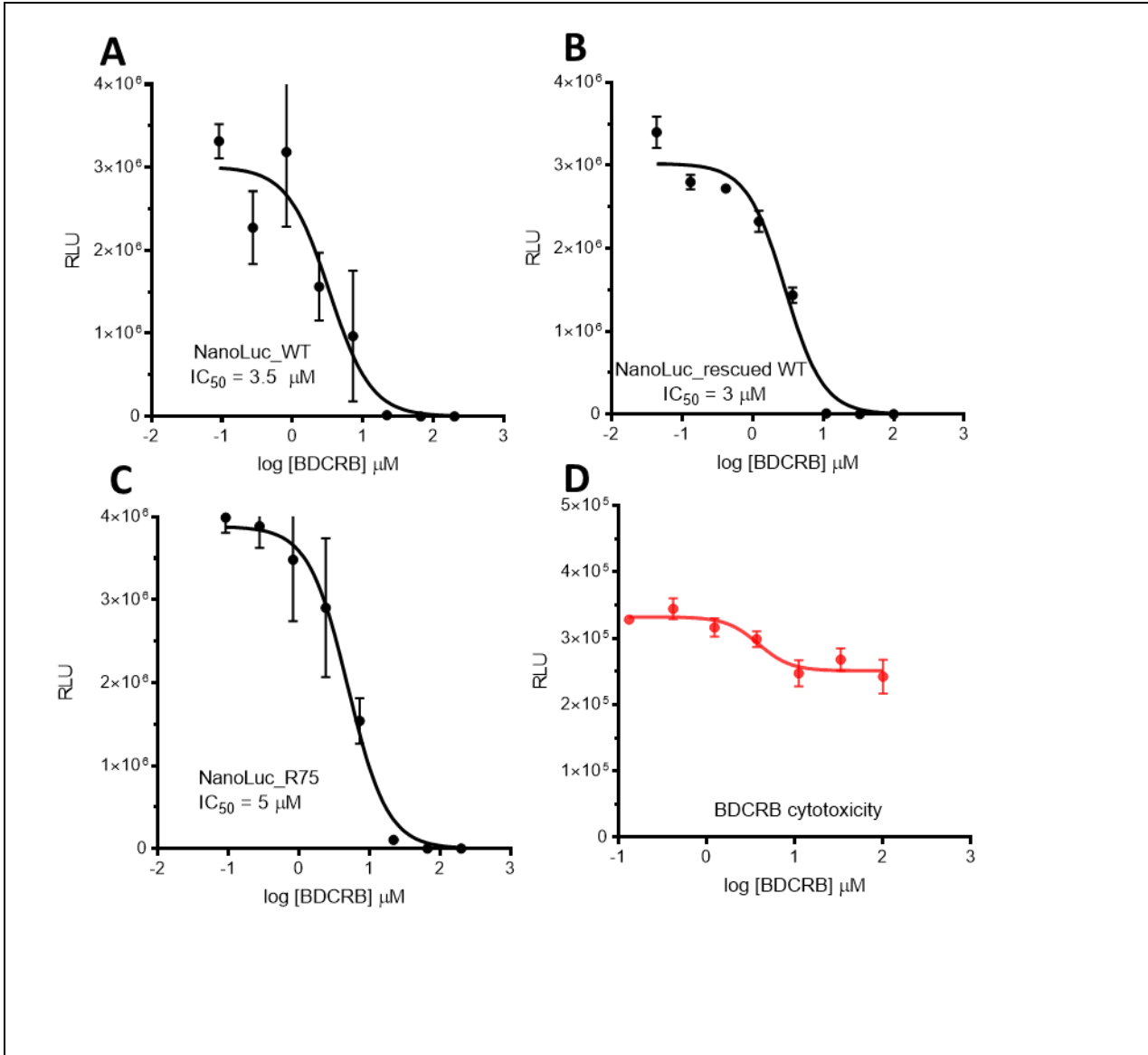**Figure 15:** The L406P mutation in GP89 does not confer significant BDCRB resistance. BAC-derived viruses A- NanoLuc-GPCMV-parental (Nano-Luc), B- NanoLuc-GPCMV-WT-rescued (Nano-Luc rescued), C- NanoLuc-GPCMV-R75 (Nano-Luc R75) and D- BDCRB cytotoxicity were assayed for sensitivity to BDCRB using the luciferase-based yield reduction assay and cytotoxicity assay.

Aim 3: Determine the antiviral activities of four highly positively charged compounds against HCMV

Four highly positively charged compounds (TriplatinNC, Pt(dien)Xan), DiplatinNC, and Werner's Complex) were hypothesized to inhibit viral entry by neutralizing negative charges of cell surface glycosaminoglycans, which are believed to mediate initial interactions of many enveloped viruses with the surface of target cells. We therefore investigated the potential activities of these four candidate compounds as antivirals against HCMV. Virus BADrUL131-Y4, a HCMV genetically engineered to express GFP, was used to develop a GFP-based assay to evaluate inhibition of HCMV spread in cultured cells. Human MRC-5 fibroblasts in 96-well plates were infected with BADrUL131-Y4 at an MOI of 0.1 and incubated in the presence of increasing concentrations of the four candidate compounds. After nine days GFP fluorescence was measured in RFU and IC_{50} values were determined as described above.

As shown in Figure 16, TriplatinNC and Pt(dien)Xan lacked detectable antiviral activity even at the highest concentrations tested (10 and 100 µM, respectively); however, DiplatinNC and Werner's Complex inhibited HCMV spread with IC_{50}s of 6.3 and 4.7 µM, respectively. Cytotoxicities were determined in parallel using uninfected cells. DiplatinNC showed no cytotoxicity at 88 µM but was highly toxic at 100 µM. The lack of additional data points at concentrations > 100 µM precluded the use of nonlinear regression to calculate a TC_{50}, but from the results the TC_{50} can be inferred to be 88 µM but < 100 µM. Thus, the selectivity index (ratio of TC_{50}/IC_{50}) for DiplatinNC is > 14. Werner's Complex exhibited no cytotoxicity at 10 µM but began to reduce cell viability at 100. Cell viability approached 50% at 100 µM, suggesting that the TC_{50} for Werner's Complex is just over 100 µM. Therefore, the selectivity index for Werner's Complex is > 32.
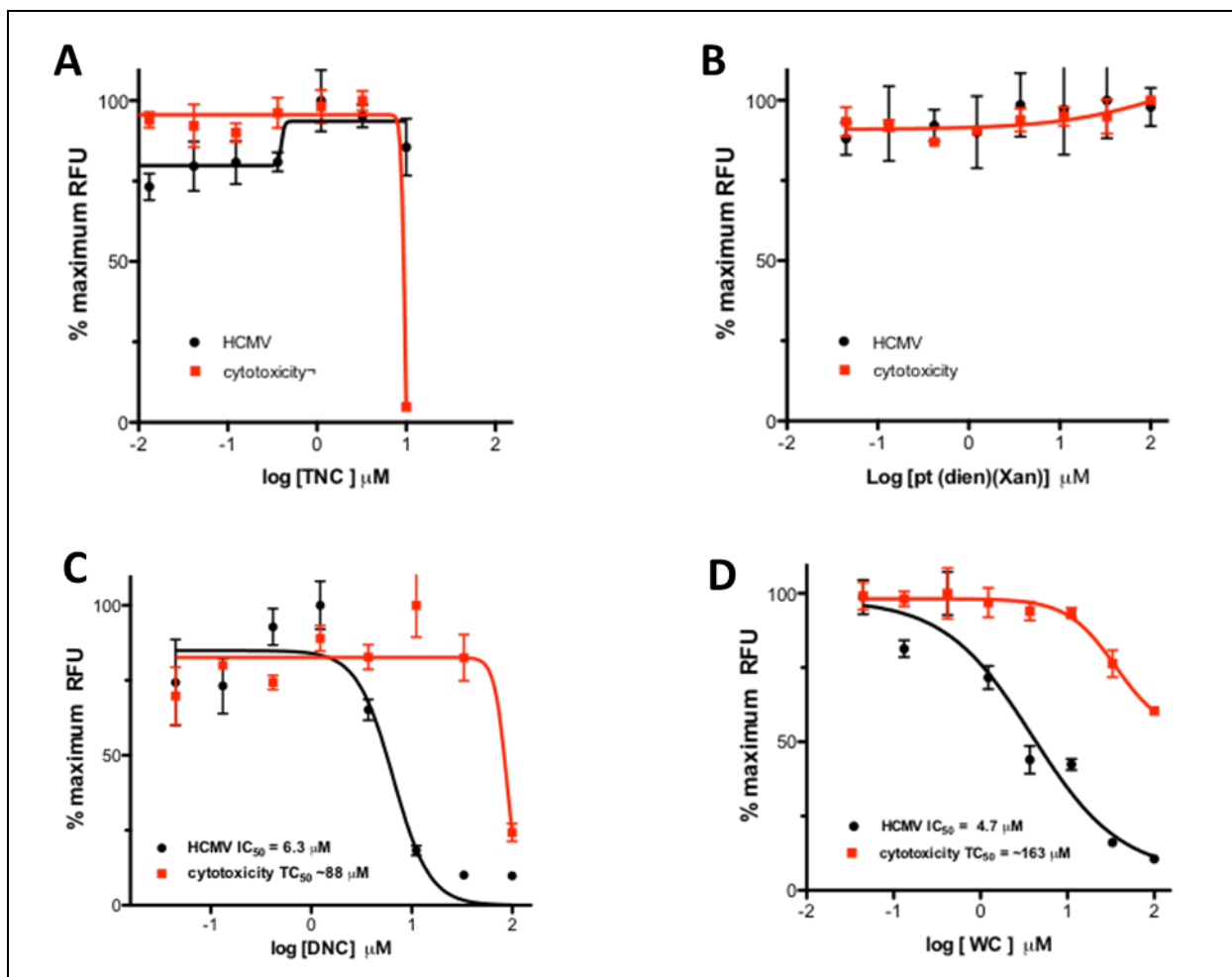
Figure 16: HCMV inhibitory activities and cytotoxicities of positively charged compounds. MRC-5 cells in 96-well plates were infected with GFP-tagged HCMV virus BAD*r*UL131-Y4 at an MOI of 0.1, then incubated in the presence of increasing concentrations of TriplatinNC (TNC) (A), Pt(dien)Xan) (B), DiplatinNC (DNC) (C), or Werner's Complex (WC) (D). GFP fluorescence in each well was measured in RFUs 9 days after infection. Cytotoxicities (red) were measured by incubating replicate uninfected MRC-5 cultures with the same range of compound concentrations for 9 days and then measuring cell viability in RLU using the CellTiter-Glo® assay. In C and D the RFUs from antiviral and RLUs from cytotoxicity experiments were normalized by converting to % maximum.

From these results, it can be concluded that although TriplatinNC and Pt(dien)Xan) are not toxic at the concentrations tested, they do not inhibit the spread of HCMV. In contrast, DiplatinNC and Werner's Complex inhibit spread of HCMV at concentrations well below their toxic levels, suggesting that each has specific antiviral activity against HCMV.

DISCUSSION

HCMV, also known as human herpes virus 5, belongs to the family *Herpesviridae.* It has a large double-stranded linear 235-kb DNA genome. The genome is encased in an enveloped icosahedral capsid surrounded by a protein matrix tegument and a lipid bilayer envelope (7). The genome is replicated by virus-encoded replication factors, including a viral DNA polymerase. All currently licensed HCMV antivirals block viral DNA synthesis by targeting the DNA polymerase. They all have serious toxicities, and mutations in the viral DNA polymerase or pUL97 lead to drug resistance. Also, they are potentially carcinogenic and teratogenic, and therefore are not approved for use during pregnancy (21,24). Drugs that do not target DNA synthesis and are non-toxic for pregnant women are needed.

Our objective in undertaking this research is to explore new antiviral targets that do not target DNA synthesis. One important new target that has emerged in recent years is the viral terminase complex, which mediates packaging of viral DNA into capsids and subsequent cleavage of the DNA to release mature viral genomes within capsids. Letermovir represents an apparent success in developing new HCMV inhibitors that target terminase. While it has not yet been licensed, it has completed phase 3 testing and the results thus far have been very encouraging. While, if licensed, letermovir will most likely be used primarily for treating transplant patients, the high potency and apparent low toxicity of letermovir make it an attractive candidate for potential future use in treating congenital HCMV infections.

An animal model with which to evaluate the efficacy of letermovir or other candidate antivirals in the context of congenital infection would be extremely helpful. However, the strict specificity of HCMV for humans precludes studies of HCMV infection in animals. The guinea

41

pig/GPCMV system is a well-established small animal model for congenital CMV transmission and pathogenesis, and can be used to evaluate antiviral efficacy, but only if the inhibitors to be tested have antiviral activity against GPCMV. Thus, in **Aim 1** we sought to evaluate both the previously tested terminase inhibitors BDCRB and BAY 38-4766, as well as letermovir, for activity against GPCMV.

The virus yield reduction assay is a powerful technique that can be used to evaluate the effectiveness of antiviral compounds. The use of viruses that express a luciferase reporter is a modern technique that provides rapid quantitative data for antiviral assays and replaces the need to determine, via plaque assay, the production and release of new virus progeny from the infected cells. Like titer-based assays, the luciferase-based assay allows the determination of antiviral activity over a wide dynamic range of more than 2 logs. But unlike titer-based assays, which require extensive serial dilutions and cell culture infectivity assays, luciferase data can be collected in a matter of minutes without need for serial dilutions.

To develop a luciferase-based antiviral assay for GPCMV we used NanoLuc-GPCMV, a genetically engineered GPCMV that was recently constructed by another member of our laboratory to contain a NanoLuc expression cassette. After initial optimization, appropriate conditions were established for the yield-reduction assay. The assay was then used to determine and evaluate the sensitivity of GPCMV to three novel inhibitory compounds that target terminase: BDCRB, BAY 38-4766, and letermovir.

Our results determined the IC_{50} against GPCMV for BDCRB to be 3.5 μM. This is very similar to the IC_{50} of 4.7 μM determined previously by titer reduction (4).We further showed, using the CellTiter-Glo® cell viability assay, that BDCRB exhibited no significant toxicity for uninfected GLF cells even at the highest concentration tested of 100 μM. Thus, although

GPCMV is less sensitive to BDCRB than HCMV (reported IC_{50} ~0.6 μM (2)) our data indicate that BDCRB does have specific antiviral activity against GPCMV that is not due to cytotoxicity. While the mechanism of action of BDCRB against GPCMV has been explored using in vitro cell culture techniques (4), it has not been investigated in vivo using the guinea pig model.

The luciferase-based assay determined the IC_{50} against GPCMV of BAY 38-4766 to be 1.1 μM, again comparable to the previously reported IC_{50}s of 0.4 to 0.6 μM determined by both plaque reduction and titer-based yeild reduction assays (27). Thus, the potency of BAY 38-4766 against GPCMV is similar to its potency against HCMV IC_{50} 1.21 ± 0.08 μM reported for HCMV (28)). Oral delivery of BAY 38-4766 (50 mg/kg/day) was well tolerated by guinea pigs and reduced both viremia and lethality of GPCMV in immunosuppressed guinea pigs (27). BAY 38-4766 did not progress to clinical testing in humans for reasons that have not been publically disclosed.

Finally, the luciferase-based assay determined the IC_{50} against GPCMV of letermovir to be 30 μM, while its reported IC_{50} for inhibition of HCMV is 6000-fold lower at 5 nM (26). While we have not measured the toxicity of letermovir or GLF cells, reported toxicity for human fibroblasts is 30 μM (42). Thus, it appears that the activity of letermovir against GPCMV, which was only observed at the highest concentration of 100 μM, is almost certainly due to cytotoxicity. Therefore, GPCMV does not appear to be sensitive to letermovir. This result is consistent with other studies that indicate letermovir is very specific for HCMV and does not inhibit other herpesviruses, including the other human herpesviruses, and mouse, rat, and rhesus cytomegalovirus (38).

In **Aim 2** we further explored the mechanism of action of BDCRB against GPCMV by evaluating a mutation in the terminase subunit GP89 that was identified by targeted genome

sequencing of a BDCRB-resistant GPCMV variant. We used *in silico* homology-based structural

modeling to construct potential structural models for UL89 and GP89, and then used the

locations of known HCMV BDCRB resistance mutations to predict where BDCRB might bind to

UL89. Both structural models were based on the crystal structure of bacteriophage T4 gp17.

Using the homology structure of UL89, a potential BDCRB binding pocket was identified near

residues D344 and A355, which confer HCMV resistance to BDCRB when mutated to E and S,

respectively (4). The *in silico* docking algorithm GOLD was the used to determine the most

favorable binding configuration of BDCRB in this putative binding pocket. Our results suggested

a significant decrease in the favorability of BDCRB binding to this pocket when UL89 contains

the D344E mutation, supporting a model in which BDCRB binds to this pocket to inhibit the

function of wild type UL89 cannot bind to a pocket containing the D344E mutation. That the

putative BDCRB binding pocket lies in a putative "hinge region" of UL89 that has been

hypothesized to flex during DNA translocation suggests a mechanism by which BDCRB inhibits

terminase function. However, identification of the analogous binding pocket within the

homology-based structure of GP89 revealed that the L406 residue is located far away in 3-D

space from the potential BDCRB-binding pocket in GP89. This result did not support a

hypothesis in which the L406P mutation in GP89 contributes to the BDCRB-resistance of

GPCMV variant R-75 by disrupting BDCRB binding to the putative binding pocket.

To conclusively determine the role of the L406 mutation in BDCRB-resistance, galK

recombineering in *E. coli* was used to insert the L406P mutation into the otherwise wild type

BDCRB-sensitive genetic background of NanoLuc-GPCMV. The results showed that the L406P

mutation did not result in a significant increase in the IC_{50} of BDCRB for GPCMV. Therefore,

we conclude that the L406P mutations does not contribute significantly to the BDCRB-resistance

of virus R75. Why the L406P mutation occurred in virus R75 is unclear. It could be a spontaneous mutation that happened by chance to be isolated during the limiting-dilution process, or it could be a compensatory mutation that somehow improves replication of R75, which may be impaired by other mutations that do confer BDCRB resistance, but does itself not provide any resistance to BDCRB. For example, that mutations in the UL104 portal protein of HCMV occur in the context of viruses encoding BDCRB-resistance mutations in UL89, but on their own do not confer BDCRB resistance (44) suggests that the resistance mutations in UL89 may hinder UL89 interactions with UL104, reducing viral replication, but this effect can be counteracted by compensatory mutations in UL104.

Thus, given that the L406P mutation has now been ruled out, the genetic basis for BDCRB-resistance of virus R75 remains unresolved. While the complete genome of R75 has not been sequenced, no other mutations were detected in GP89 or GP56. GP51, homolog of HCMV UL51, has not yet been sequenced in virus R75, as at the time that the sequencing studies were carried out herpesvirus terminases were thought to contain only two subunits (UL89 and UL56 in the case of HCMV). However, since identification of UL51 as a third terminase subunit, no mutations in UL51 or its homologs in other Cytomegalovirus have been identified in viruses with resistance to BDCRB, other halogenated benzimidazoles, BAY 38-4766, or letermovir. Beside the L406P mutation, two additional genetic anomalies have been described in R75 that could contribute to BDCRB resistance: a 12-kb deletion in the Hind III E region, and accumulation of a large number of terminal repeats at either end of the genome. That the 12-kb deletion contributes to BDCRB resistance is unlikely, given that a mutant GPCMV variant designated BVD has an overlapping and slightly larger deletion and lacks all the genes that are missing from this region of R75 (Sauer and McVoy, unpublished), yet is sensitive to BDCRB (Figure 13)

Thus, it may be that the large number of terminal repeats in R75 may confer BDCRB-resistance. One simple hypothesis for a mechanism of resistance is that if BDCRB reduces the efficiency with which terminase recognizes the *cis*-acting cleavage site sequences, the increased number of terminal repeats, each containing these *cis* cleavage site sequences, may simply give terminase more opportunities to recognize and cleave the DNA, thus increasing the probability of productive cleavage events occurring. Future studies should include sequencing the full genome of R75 to determine if potential mutations exist in GP51, GP104 (portal) or other loci in the genome, and evaluation of the genomic termini of NanoLuc-GPCMV-R75 to determine if perhaps the L406P mutation may have promoted accumulation of additional terminal repeats in this virus. If the latter is the case, an increased number of terminal repeats can be ruled out as contributing to BDCRB resistance. Interestingly, the hypothesis that the number of terminal repeats may have increased in response to the 12-kb deletion, which would allow the number of repeats to increase without exceeding the normal overall genome length, appears to be incorrect, as the BVD genome has the normal one or zero copies of terminal repeats found on wild type GPCMV (Sauer and McVoy, unpublished observations).

Lastly, in **Aim 3**, potential novel inhibitors of HCMV were investigated. Four highly positively charged compounds (TriplatinNC, Pt(dien)Xan), DiplatinNC, and Werner's Complex) were hypothesized to inhibit viral entry by neutralizing negative charges of cell surface glycosaminoglycans, which are believed to mediate initial interactions of many enveloped viruses with the surface of target cells. Using a GFP-based viral spread assay, DiplatinNC and Werner's Complex were found to have significant antiviral activity with corresponding low toxicity. That both TriplatinNC and Pt(dien)Xan) lacked activity in this assay suggests that charge alone is not sufficient for antiviral activity, as on this basis all four compounds were

equally predicted to inhibit viral entry by neutralizing negative charges of cell surface glycosaminoglycans. Thus, either TriplatinNC and Pt(dien)Xan) are somehow ineffective a neutralizing change on the appropriate cell surface factors, or DiplatinNC and Werner's Complex may have different mechanisms of action from that proposed. Further studies are needed to characterize the mechanisms of action of DiplatinNC and Werner's Complex. In particular, time of addition and removal studies can be designed to determine if these compounds act by blocking HCMV attachment to or entry into cells, or if they act at later stages of viral replication, including disrupting specific stages of the viral gene expression cascade, viral DNA replication, genome cleavage and packaging, or final stages of virion tegumentation, envelopment, and egress.

Terminase is a novel and attractive target for antiviral development. Several HCMV anti-viral inhibitors targeting terminase have been identified, but only one, letermovir (AIC246), has progressed in clinical development and has recently completed phase 3 testing. The structure and functions of terminase are poorly understood and consequently the mechanisms of action of all three classes of terminase inhibitors are uncertain. One important weakness is the absence of complete molecular structures for HCMV terminase subunits UL89, UL56, and UL51, or their homologs in other herpesviruses. A better understanding the terminase structure and the functions of individual subunits and complexes is important for understanding the process of DNA packaging and for future development of antivirals targeting terminase.

While DiplatinNC and Werner's Complex may not have significant potential for clinical development, they may represent novel mechanisms by which small molecules can interfere with HCMV replication. As such, they may serve as valuable pharmacological probes to discover and elucidate novel antiviral targets and/or mechanisms of inhibition that could lead to development

of new classes of effective and nontoxic antivirals for the treatment of HCMV and potentially

other viruses.

V. REFERENCES

1.   Champier, G., S. Hantz, A. Couvreux, S. Stuppfler, M. C. Mazeron, S. Bouaziz, F. Denis, and S. Alain. 2007. New functional domains of human cytomegalovirus pUL89 predicted by sequence analysis and three-dimensional modelling of the catalytic site DEXDc. Antivir Ther 12:217-232.

2.   Underwood, M. R., R. J. Harvey, S. C. Stanat, M. L. Hemphill, T. Miller, J. C. Drach, L. B. Townsend, and K. K. Biron. 1998. Inhibition of human cytomegalovirus DNA maturation by a benzimidazole ribonucleoside is mediated through the UL89 gene product. J Virol 72:717-725.

3.   Krosky, P. M., M. R. Underwood, S. R. Turk, K. W. Feng, R. K. Jain, R. G. Ptak, A.C. Westerman, K. K. Biron, L. B. Townsend, and J. C. Drach. 1998. Resistance of Human cytomegalovirus to benzimidazole ribonucleosides maps to two open reading frames: UL89 and

4.   Nixon DE, McVoy MA. 2004 Dramatic effects of 2-bromo-5,6-dichloro-1-beta-D-ribofuranosyl benzimidazole riboside on the genome structure, packaging, and egress of guinea pig cytomegalovirus. J Virol. 2004 Feb; 78(4):1623-35.

5.   Sheri Lewis Bate, Sheila C. Dollard, Michael J. Cannon; Cytomegalovirus Seroprevalence in the United States: The National Health and Nutrition Examination Surveys, 1988–2004. Clin Infect Dis 2010; 50 (11): 1439-1447. doi: 10.1086/652438

6.   Boeckh M, Geballe AP. Cytomegalovirus: pathogen, paradigm, and puzzle. J Clin Invest. 2011;121((5)):1673–80

7.   Andhi MK, Khanna R. Human cytomegalovirus: clinical aspects, immune regulation, and emerging treatments. Lancet Infect Dis. 2004;4((12)):725–38

8.	V.C. Emery and P.D. Griffiths. 1990. Current Status Review Molecular biology of cytomegalovirus. Int. J. Exp. Path. 71:905-9I8.

9.	Peter A, Telkes G, Varga M, Jaray J. 2008. Gastrointestinal cytomegalovirus infections in organ transplant patients. Orv Hetil. 149(52):2463-70.

10.	Mariagabriela Alterio de Goss, Rafaela Holtappels, Hans-Peter Steffens, Jürgen Podlech, Peter Angele, Liane Dreher,Doris Thomas, and Matthias J. Reddehase. 1998. Control of Cytomegalovirus in Bone Marrow Transplantation Chimeras Lacking the Prevailing Antigen-Presenting Molecule in Recipient Tissues Rests Primarily on Recipient-Derived CD8 T Cells. J Virol. 72(10):7733–7744.

11.	Irene G. Sia and Robin Patel. 2000. New Strategies for Prevention and Therapy of Cytomegalovirus Infection and Disease in Solid-Organ Transplant Recipients. Clin Microbiol Rev. 13(1):83–121.

12.	Van Der Bij W, et al. (2001). Management of cytomegalovirus infection and disease after solid-organ transplantation. Clinical Infectious Disease, 33(7), 532-537.

13.	Jab DA (1996). Treatment of cytomegalovirus retinitis in patients with AIDS. Annals of Internal Medicine, 125, 144-145.

14.	Sugar EA, Jabs DA, Ahuja A, Thorne JE, Danis RP, Meinert CL. 2012. Studies of the Ocular Complications of AIDS Research Group. Incidence of cytomegalovirus retinitis in the era of highly active antiretroviral therapy. Am J Ophthalmol. 153(6):1016-1024.

15.	Sugawara M, et al. (2000). Transport of valganciclovir, a ganciclovir prodrug, via peptide transporters PEPT1 and PEPT2. Journal of Pharmaceutical Sciences, 89(6), 781-790.

16.	Griffiths PD, et al. (1984). A prospective study of primary cytomegalovirus infection during pregnancy: Final report. British Journal of Obstetrics and Gynaecology, 91, 307-315.

17.   Adler SP. 2005. Congenital cytomegalovirus screening. Pediatr Infect Dis J. 24(12):1105-6.

18.   Nelson CT, et al. (1997). Cytomegalovirus infection in the pregnant mother, fetus, and newborn infant. Clinics in Perinatology, 24(1), 151-160.

19.   Biron KK (2006). Antiviral drugs for cytomegalovirus disease. Antiviral Research, 71, 154-160.

20.   Barnard DL, et al. (1995). Anti-human cytomegalovirus activity and toxicity of sulfonated anthraquinones and anthraquinone derivatives. Antiviral Research, 28(4), 317-329.

21.   Barnard DL, et al. (1992). Evaluation of the antiviral activity of anthraquinones, anthrones, and anthraquinone derivatives against human cytomegalovirus. Antiviral Research, 1, 63-77.

22.   Mettenleiter et al. 2008. "Molecular Biology of Animal Herpesviruses". Animal Viruses: Molecular Biology. Caister Academic Press. ISBN 1-904455-22-0

23.   Kehm, E., MA Gosku and CW Knopf. 1998. Expression analysis of recombinant herpes simplex virus type 1 DNase. Virus Genes. 17:129-138.

24.   Field AK. 1999. Human cytomegalovirus: challenges, opportunities and new drug development. Antivir Chem Chemother. 10(5):219-32.

25.   Biron, K.K. 2006. Antiviral drugs for cytomegalovirus disease. Antiviral research. 71:154-16.

26.   Goldner, et all. (2011). The Novel Anticytomegalovirus Compound AIC246 (Letermovir) Inhibits Human Cytomegalovirus Replication through a Specific Antiviral Mechanism That Involves the Viral Terminase . Journal of Virology, 85(20), 10884–10893.

27.   Schleiss, et all. (2005). The non-nucleoside antiviral, BAY 38-4766, protects against cytomegalovirus (CMV) disease and mortality in immunocompromised guinea pigs. *Antiviral Research*, *65*(1), 35–43.

28.   Buergeret all. (2001). A Novel Nonnucleoside Inhibitor Specifically Targets Cytomegalovirus DNA Maturation via the UL89 and UL56 Gene Products. *Journal of Virology*, *75*(19), 9077–9086.

29. Wang D, *et al.* (2004). Human cytomegalovirus encodes a highly specific RANTES decoy receptor. *Proceedings of the National Academy of Sciences of the United States of America, 101*(47), 16642-16647.

30. Townsend, L. B., R. V. Devivar, S. R. Turk, M. R. Nassiri, and J. C. Drach. 1995. Design, synthesis, and antiviral activity of certain 2,5,6-trihalo-1-(beta-Dribofuranosyl) benzimidazoles. J Med Chem 38:4098-4105.

31. Cui X, McGregor A, Schleiss MR, McVoy MA. 2008. Cloning the complete guinea pig cytomegalovirus genome as an infectious bacterial artificial chromosome with excisable origin of replication. J Virol Methods 149:231–239. doi: 10.1016/j.jviromet.2008.01.031

32.   Warming S, Costantino N, Court DL, Jenkins NA, Copeland NG. 2005. Simple and highly efficient BAC recombineering using galK selection. Nucleic Acids Res 33: e36. doi:10.1093/nar/gni035.

33. J. Anderson-H.-G Kräusslich-Ralf Bartenschlager - Antiviral strategies. Page 167. Springer - 2009

34. Nigro G. 2009. Maternal-fetal cytomegalovirus infection: from diagnosis totherapy. J Matern Fetal Neonatal Med. 22(2):169-74.

35.   Buerger, I., Reefschlaeger, J., Bender, W., Eckenberg, P., Popp, A., Weber, O.

Hallenberger, S. (2001). A Novel Nonnucleoside Inhibitor Specifically Targets Cytomegalovirus

DNA Maturation via the UL89 and UL56 Gene Products. *Journal of Virology*, *75*(19), 9077–

9086.

36.   Padilla-Carlin, D. J., McMurray, D. N., & Hickey, A. J. (2008). The Guinea Pig as a Model

of Infectious Diseases. *Comparative Medicine*, *58*(4), 324–340.

37.   Schleiss, M. R. 2002. Animal models of congenital cytomegalovirus infection: an overview

of progress in the characterization of guinea pig cytomegalovirus (GPCMV). J Clin Virol 25

Suppl 2: S37-49.

38. Marschall, M., Stamminger, T., Urban, A., Wildum, S., Ruebsamen-Schaeff, H.,

Zimmermann, H., & Lischka, P. (2012). *In Vitro* Evaluation of the Activities of the Novel

Anticytomegalovirus Compound AIC246 (Letermovir) against Herpesviruses and Other Human

Pathogenic Viruses. *Antimicrobial Agents and Chemotherapy*, *56*(2), 1135–1137.

39.   Bhave, S., Elford, H., & McVoy, M. A. (2013). Ribonucleotide reductase inhibitors

hydroxyurea, didox, and trimidox inhibit human cytomegalovirus replication *in vitro* and

synergize with ganciclovir. *Antiviral Research*, *100*(1), 10.1016/j.antiviral.2013.07.016.

40. Silva, H., Frézard, F., Peterson, E. J., Kabolizadeh, P., Ryan, J. J., & Farrell, N. P. (2012).

heparan sulfate proteoglycan-mediated entry pathway for charged tri-platinum compounds.

differential cellular accumulation mechanisms for platinum. molecular pharmaceutics, 9(6),

1795.41. McVoy, M. A., Wang, J. B., Dittmer, D. P., Bierle, C. J., Swanson, E. C., Fernández-

Alarcón, C., … Schleiss, M. R. (2016). Repair of a Mutation Disrupting the Guinea Pig

Cytomegalovirus Pentameric Complex Acquired during Fibroblast Passage Restores

Pathogenesis in Immune-Suppressed Guinea Pigs and in the Context of Congenital Infection. *Journal of Virology*, *90*(17), 7715–7727.

42.   Hwang JS, Bogner E. ATPase activity of the terminase subunit pUL56 of human cytomegalovirus. J Biol Chem. 2002 Mar 1;277(9):6943-8. Epub 2001 Dec 13.

43. Chou, S. (2015). Rapid In Vitro Evolution of Human Cytomegalovirus UL56 Mutations That Confer Letermovir Resistance. Antimicrobial Agents and Chemotherapy, 59(10), 6588–6593.

44. Komazin, G., Townsend, L. B., & Drach, J. C. (2004). Role of a Mutation in Human Cytomegalovirus Gene UL104 in Resistance to Benzimidazole Ribonucleosides. Journal of Virology, 78(2), 710–715.

45. Evers, D. L., Komazin, G., Ptak, R. G., Shin, D., Emmer, B. T., Townsend, L. B., & Drach, J. C. (2004). Inhibition of Human Cytomegalovirus Replication by Benzimidazole Nucleosides Involves Three Distinct Mechanisms. Antimicrobial Agents and Chemotherapy, 48(10), 3918–3927.

46.Emery and Hassan-Walker. Focus on new drugs in development against human cytomegalovirus. Drugs 2002; 62:1853-1858

47. Lyndsey J. Bowman, Jennifer Iuppa Melaragno & Daniel C. BrennanLetermovir for the management of cytomegalovirus infection. Expert Op Invest Drugs 2017; 26:235-241}

VITA

Amine Ourahmane
ourahmanea@vcu.edu

Amine Ourahmane was born on March 1, 1981, in Setif, Algeria and is an American and Algerian citizen. He graduated from Setif High School (Algeria) in 1999. He received his Bachelor in Microbiology from Farhat Abbas (Setif, Algeria) in 2003 then another Bachelor of Science in Biology in 2013 from Virginia Commonwealth University, Richmond, Virginia.